

# Age and origin of the gabbros in the Jilotlán pluton, Jalisco: primitive magmatic rocks in the southern part of the Guerrero terrane

Daniel Villanueva-Lascurain<sup>1\*</sup>, Gabriela Solís-Pichardo<sup>2</sup>, Peter Schaaf<sup>3</sup>,  
Teodoro Hernández-Treviño<sup>3</sup>, Josué Salazar-Juárez<sup>4</sup>, and Pedro Corona-Chávez<sup>5</sup>

<sup>1</sup> Posgrado en Ciencias de la Tierra, Instituto de Geofísica,  
Universidad Nacional Autónoma de México, 04510 México, D.F., Mexico.

<sup>2</sup> Laboratorio Universitario de Geoquímica Isotópica (LUGIS), Instituto de Geología,  
Universidad Nacional Autónoma de México, 04510 México, D.F., Mexico.

<sup>3</sup> Laboratorio Universitario de Geoquímica Isotópica (LUGIS), Instituto de Geofísica,  
Universidad Nacional Autónoma de México, 04510 México, D.F., Mexico.

<sup>4</sup> Posgrado en Ciencias de la Tierra, Instituto de Geología,  
Universidad Nacional Autónoma de México, 04510 México, D.F., Mexico.

<sup>5</sup> Instituto de Investigaciones en Ciencias de la Tierra,  
Universidad Michoacana de San Nicolás de Hidalgo, 58060 Morelia, Mich., Mexico.

\* dangeologo@gmail.com

## ABSTRACT

An outstanding feature of the Mexican Cordilleran magmatic arc between Sonora and Chiapas is the presence of numerous plutonic and batholithic bodies of Cretaceous to Miocene ages. In this contribution, we investigated the petrogenesis and age of the gabbros from Jilotlán, Jalisco, in order to better understand their genetic relation with the intruding and surrounding Late Cretaceous calc-alkaline mantle-type granitoids. Gabbros from Manzanillo (Colima), Tepalcaltepec, and Aquila (Michoacán) were also studied. The objective of this work is to contribute new findings to the tectonic setting and magma generation processes of the Cretaceous magmatic arc in the coastal Zihuatanejo terrane, which is part of the Guerrero terrane.

All gabbros are hornblende rich, which indicates hydrated conditions. Clinopyroxene crystals and hornblende pseudomorphs have plagioclase inclusions, suggesting exsolution by a rapid uplift. Geochemically, most gabbros are calc-alkaline. The relatively flat trace element patterns display incompatible element (LILE and LREE) enrichment relative to the less incompatible elements (HFSE and HREE), which show minor enrichment or are even depleted with respect to N-MORB. Positive Pb and Sr anomalies as well as LILE enrichment in comparison to HFSE and REE suggest a magmatic arc origin.

The Sr and Nd isotopic compositions indicate that the Jilotlán, Tepalcaltepec, and Manzanillo gabbros have a common source, comparable to N-MORB. Depleted mantle model ages ( $T_{DM}$ ) are similar for the gabbros and a quartz monzodiorite (averaging ~500 Ma) reflecting participation of a crustal component in their genesis. Isotopic data indicate that the gabbros could have been generated from a combination of mantle and crustal components. The existence of a Cretaceous, Barremian to Albian (~130–100 Ma), extensional arc proposed by other studies suggests that the gabbros were generated in a thinned crust setting.

Hornblende <sup>40</sup>Ar/<sup>39</sup>Ar ages and U-Pb zircon ages of Jilotlán gabbros are undistinguishable at ~114 Ma, which indicates that they crystallized ~40 Ma earlier than the surrounding granitoids dated at ~70 Ma. The identical ages for both isotopic systems in the gabbros give evidence for their shallow emplacement and/or rapid uplift. The ~118 Ma (K-Ar hornblende) age of an andesite from the Tecalitlán Formation host rock suggests that the gabbros may represent the plutonic counterpart of this volcanosedimentary sequence.

The crystalline rocks of the study area are magmatically very primitive (initial epsilon Nd ( $\epsilon Nd_i$ ) up to ~+7,  $T_{DM}$  max. ~0.7 Ga), without evidence of evolved crustal components in comparison to the Puerto Vallarta batholith, located NW of the study area, which contains Precambrian crustal components ( $\epsilon Nd_i$  as low as ~-7,  $T_{DM}$  up to ~1.55 Ga). This evidences different tectonic settings for these two areas. This study supports the hypothesis that a long-lived subduction zone (at least since the Early Cretaceous) generated poorly evolved arc rocks in a continental arc setting in the Guerrero terrane.

Key words: gabbro; petrogenesis; geochronology; Jilotlán pluton; Guerrero terrane; Mexico.

## RESUMEN

*Un rasgo sobresaliente del arco magmático Cordillerano Mexicano, entre Sonora y Chiapas, es la presencia de numerosos cuerpos plutónicos y batolíticos con edades del Cretácico al Mioceno. En esta contribución investigamos la petrogénesis y las edades de los gabros de Jilotlán, Jalisco, para entender mejor su relación con los plagiogranitos calco-alcálicos del Cretácico Superior que los intrusionan y que son aledaños. Gabros de Manzanillo (Colima), Tepalcaltepec y Aquila (Michoacán) también fueron estudiados. El objetivo de este trabajo es contribuir con nuevos*

datos al contexto tectónico regional y a los procesos de generación de magmas del arco magmático Cretácico en la parte costera del terreno Zihuatanejo, parte del terreno Guerrero.

Todos los gabros son ricos en hornblenda, lo que indica condiciones hidratadas. Cristales de clinopiroxeno y pseudomorfo de hornblenda contienen inclusiones de plagioclasa, lo que sugiere exsolución por un ascenso rápido. Geoquímicamente, la mayoría de los gabros son calcoalcalinos. Los patrones relativamente planos de elementos traza muestran un enriquecimiento en elementos incompatibles (LILE y LREE) respecto a los elementos menos incompatibles (HFSE y HREE) que muestran menor enriquecimiento o incluso empobrecimiento con respecto a N-MORB. Anomalías positivas de Pb y Sr así como el enriquecimiento en LILE a comparación con HFSE y REE sugieren un origen de arco magmático.

Las composiciones isotópicas de Sr y Nd indican que los gabros de Jilotlán, Tepalcatepec y Manzanillo tienen una fuente común, comparable a N-MORB. Las edades modelo  $T_{DM}$  son similares para los gabros y una cuarzomonzodiorita (~500 Ma en promedio) reflejando la participación de un componente cortical en su generación. Los datos isotópicos indican que los gabros pudieron generarse a partir de una combinación de manto y componentes corticales. La existencia de un arco extensional cretácico del Barremiano al Albiano (~130–100 Ma) propuesto en otros estudios, sugiere que los gabros fueron generados en un escenario de corteza adelgazada.

Las edades de  $^{40}\text{Ar}/^{39}\text{Ar}$  en hornblenda y U-Pb en zircones de los gabros de Jilotlán son indistinguibles en ~114 Ma, lo que indica que su cristalización ocurrió ~40 Ma antes que la de los granitoides aledaños fechados en 70 Ma. La edad idéntica de los gabros en ambos sistemas isotópicos da evidencia de su emplazamiento somero y/o ascenso rápido. La edad de ~118 Ma (K-Ar en hornblenda) de una andesita de la roca encajonante de la Formación Tecalitlán, sugiere que los gabros pueden ser la contraparte plutónica de esta secuencia volcanosedimentaria.

Las rocas cristalinas del área de estudio son magmáticamente muy primitivas ( $\epsilon\text{Nd}_i$  ~+7,  $T_{DM}$  máx. ~0.7 Ga) sin componentes corticales evolucionados en comparación con el batolito de Puerto Vallarta, al NW del área de estudio, que contiene componentes corticales del Precámbrico ( $\epsilon\text{Nd}_i$  ~-7,  $T_{DM}$  hasta ~1.55 Ga). Esto evidencia un límite tectónico entre las dos áreas. Este estudio apoya la hipótesis de que una zona de subducción de larga vida (por lo menos del Cretácico Temprano) generaba rocas magmáticas primitivas en un escenario de arco continental en el terreno Guerrero.

**Palabras clave:** gabros; petrogénesis; geocronología; plutón de Jilotlán; terreno Guerrero; México.

## INTRODUCTION

Gabbros and associated mafic rocks are significant constituents of many calc-alkaline granitoids and abundant in numerous Cordilleran plutons (e.g., Barbarin, 2005; Kimbrough *et al.*, 2015). Understanding their petrogenesis provides relevant information about the role of mafic magmas in the generation and evolution of the Earth's crust.

The acquisition of reliable isotopic and geochronologic data of magmatic rocks is a key for determining the nature of the basement of tectonostratigraphic terranes in Mexico. In this paper, we report on gabbroic rocks found within mantle-type granite near Jilotlán, Jalisco, in the central part of the belt of Cretaceous Cordilleran plutons of Mexico (Figure 1a). This plutonic and batholithic belt extends from Baja California to Oaxaca parallel to the Pacific coast with NW-SE decreasing Late Cretaceous to early Miocene ages (~103–20 Ma) obtained by various geochronologic methods. In Jalisco, Colima and Michoacán the plutonic bodies and some associated volcanic rocks

show in general Late Cretaceous to Paleocene ages (Gastil *et al.*, 1978; Pantoja-Alor, 1983; Grajales-Nishimura and López-Infanzón, 1984; Schaaf, 1990; Schaaf *et al.*, 1995; Morán-Zenteno *et al.*, 2000; 2005; Ferrari *et al.*, 2014). The predominant position of the plutonic belt close to the Pacific coast evidences a continental margin truncation that indicates intensive tectonic processes from the Late Cretaceous to the early Miocene in western Mexico, including forearc removal by subduction erosion (Malfait and Dinkelman, 1972; Schaaf *et al.*, 1995; 2000; Schaaf, 2002; Morán-Zenteno *et al.*, 2005).

The study area is located in the Zihuatanejo terrane (Figure 1b), a part of the Guerrero composite terrane (Campa and Coney, 1983). The limits and evolution of the Guerrero terrane are still under discussion, because of its complex and variable stratigraphy and its large extension (Centeno-García *et al.*, 2008; Figure 1b). In this contribution, we integrate petrographic, geochemical, isotopic, and geochronologic data in order to understand the magmatic origin of the Jilotlán gabbros and their relationship to the surrounding mantle-type granites. The results of this work contribute to the understanding of the nature of the crust in the eastern Guerrero terrane, its evolution, and tectonic setting in the late Early Cretaceous to Paleogene time span.

## GEOLOGIC SETTING

### Guerrero terrane

The Guerrero terrane was first defined by Campa and Coney (1983) as a composite terrane conformed by submarine volcanic and sedimentary sequences of Late Jurassic to middle Cretaceous age and a report of Upper Triassic rocks near Zacatecas. The aforementioned authors divided the Guerrero terrane into three subterrane (Teloloapan-Ixtapan, Zihuatanejo, and Huetamo), based on different stratigraphic features, metamorphic grade, and deformational style. The terrane was later named Náhuatl Terrane by Sedlock *et al.* (1993), characterized by deformed and metamorphosed Jurassic to Cretaceous magmatic and sedimentary rocks of continental and marine affinity with a probable occurrence of Paleozoic rocks in the eastern part of the terrane. The Náhuatl terrane corresponds to the southern part of the Guerrero terrane of Campa and Coney (1983). Referring to both nomenclatures, a main difference is that the Guerrero-Morelos platform is included in the Náhuatl Terrane, whereas it is not included in the Guerrero Terrane (Elías-Herrera *et al.*, 2000).

Further studies, based on stratigraphic and geochemical data, subdivided the Guerrero terrane into the Tahue, Zihuatanejo, Guanajuato, Arcelia, and Teloloapan terranes (Centeno-García *et al.*, 1993, 2003, 2008; Talavera *et al.*, 1995; Mendoza and Suástegui, 2000; Centeno-García, 2005) with volcanic and sedimentary marine successions, and minor subaerial Upper Jurassic (Tithonian) to middle-Upper Cretaceous (Cenomanian) sequences (Centeno-García *et al.*, 2003). Some scarce Paleozoic units were also reported (Centeno-García, 2005; Centeno-García *et al.*, 2008).

### Nature of the Guerrero terrane

Some authors emphasized the autochthonous character of the Guerrero terrane, which was predominantly built on continental crust (De Cserna, 1978; De Cserna *et al.*, 1978). Others described it as a para-autochthonous marine volcanosedimentary sequence, polydeformed and metamorphosed to greenschist facies, with continental arc affinity and evidence of continental crust in its southern part (Elías-Herrera and Sánchez-Zavala, 1992; Elías-Herrera and Ortega-Gutiérrez, 1997; Elías-Herrera *et al.*, 2000). Less current models proposed it as an allochthonous terrane, consisting of a distant oceanic island arc that would have collided with North America during the late Early Cretaceous

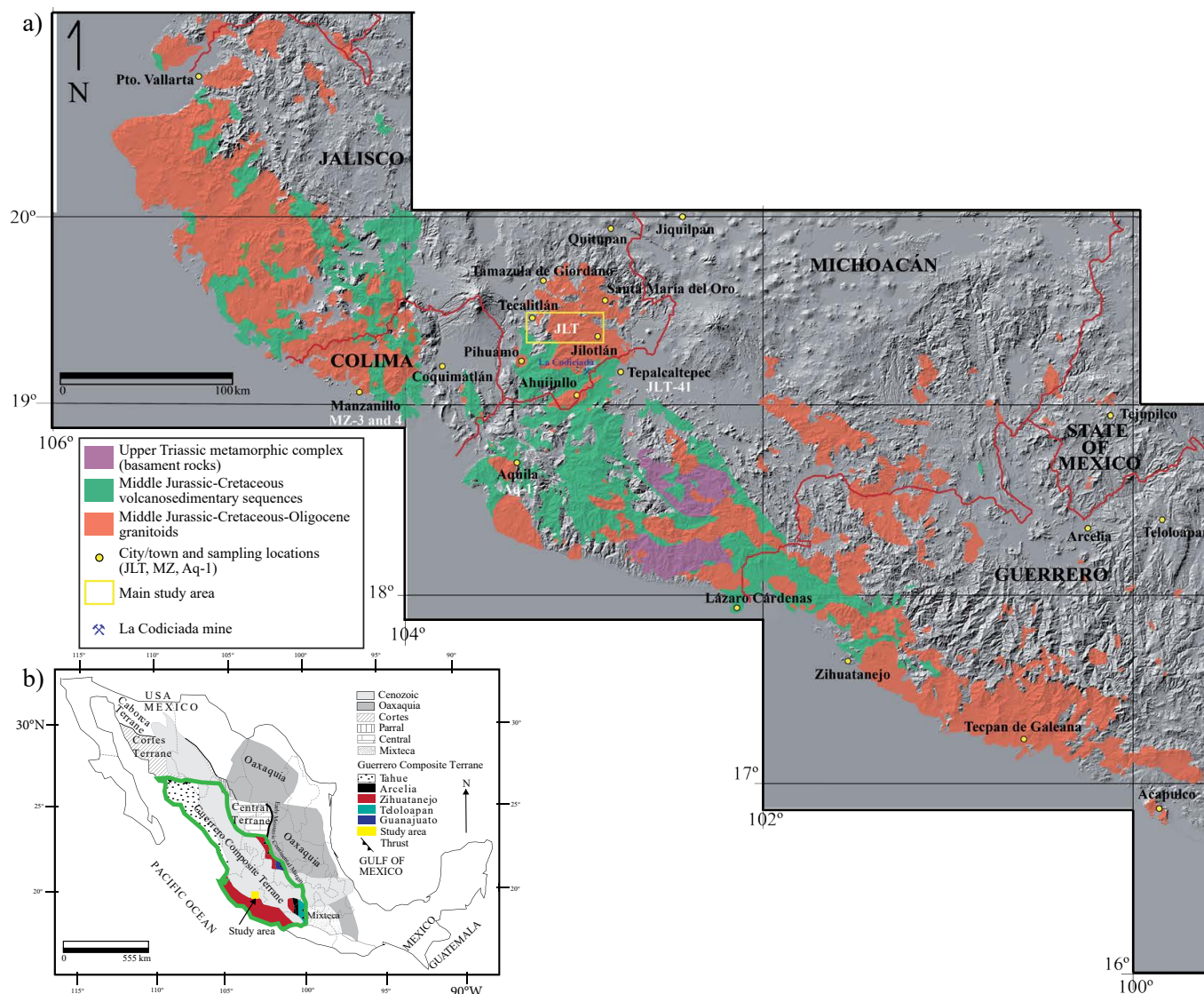


Figure 1. a) Regional geologic map showing the distribution of plutons, volcanic and basement rocks between Puerto Vallarta and Acapulco (modified from Carta Geológica de la República Mexicana del Servicio Geológico Mexicano, 2007, escala 1: 2,000,000); using digital elevation models from the Instituto Nacional de Estadística y Geografía (INEGI). The location of the study area is shown as well as the Tepalcaltepec and Manzanillo sampling locations. b) Location of the Guerrero Terrane, in relation to other tectonostratigraphic terranes of Mexico (from Centeno-García *et al.*, 2008).

(Lapierre *et al.*, 1992) or the Late Cretaceous (Tardy *et al.*, 1994), and would have closed an ocean basin. Another study suggested that the ocean basin had two subduction zones, verging east and west, before the easterly travelling arc finally closed the basin and was accreted to North America during the Early Cretaceous (Dickinson and Lawton, 2001).

Most authors define the Guerrero terrane as a complex system of one, two or three peripheral arcs, that developed relatively close to the continent (Campa and Coney, 1983; Elías-Herrera and Sánchez-Zavala, 1992; Centeno-García *et al.*, 1993, 2003; Elías-Herrera *et al.*, 2000; Mendoza and Suástegui, 2000; Centeno-García, 2005; Talavera *et al.*, 2007), unseparated (Elías-Herrera and Sánchez-Zavala, 1992; Centeno-García *et al.*, 1993, 2003, 2008; Elías-Herrera *et al.*, 2000; Centeno-García, 2005; Martini *et al.*, 2009), or separated by one or more subduction zones (Mendoza and Suástegui, 2000; Talavera *et al.*, 2007) throughout its evolution.

The oldest basement of the Guerrero terrane is composed of Paleozoic crust, probably of oceanic arc affinity in the northwest-

ern section (Tahue terrane), and a Triassic deep ocean basin with contemporaneous rift magmatism in the central part (Zihuatanejo terrane), which was accreted to mainland Mexico during the Early Jurassic (Centeno-García, 1994, 2005; Centeno-García and Silva, 1997; Centeno-García *et al.*, 2003, 2008). Upon this accretionary complex, one or more middle to upper Mesozoic arc(s) evolved (Centeno-García *et al.*, 1993; Elías-Herrera *et al.*, 2000; Mendoza and Suástegui, 2000).

#### Zihuatanejo terrane

The study area is located in the southern part of the Zihuatanejo terrane, the largest Guerrero subterrane (Centeno-García *et al.*, 2008 and references therein). This terrane was formed by the accretion of fringing terranes produced by extensional (rifting) and compressional (accretion) processes in the upper plate (Centeno-García *et al.*, 2011) of a single long-lived subduction zone (Centeno-García *et al.*, 1993, 2008) that dipped eastward underneath the Mexican continental margin (Martini *et al.*, 2009; Centeno-García *et al.*, 2011). The oldest rocks

found so far are located near the city of Zacatecas (Zacatecas Fm.) to the north, as well as in Huetamo and Arteaga, Michoacán (Arteaga complex) and in Las Ollas, Guerrero (Las Ollas complex) in the south (Centeno-García, 2005 and references therein; Centeno-García *et al.*, 2008 and references therein). These sequences are composed of Triassic ocean floor assemblages, which were deformed and metamorphosed during the Early to Middle Jurassic.

#### *Basement of the Zihuatanejo terrane in the study area*

The basement rocks in the study area are probably similar to those of the Arteaga complex, which is composed of tectonically imbricated quartz-rich turbidites (Centeno-García *et al.*, 2008 and references therein). According to Centeno-García (2005), the turbidites include siliciclastics, green volcanoclastics, pillow basalts, diabase, gabbros, black and green chert, and large recrystallized limestone olistoliths (Centeno-García, 1994; Centeno-García *et al.*, 2003). The siliciclastics are interbedded with thick green layers, which are interpreted as metavolcaniclastics derived from a primitive arc source and/or Mid Ocean Ridge Basalts (MORB). Pillow lavas also show geochemical and isotopic compositions similar to MORB (Centeno-García *et al.*, 1993, 2003). The whole sequence is at least ~1500 m thick and its deposition time is constrained by one Late Triassic (Ladinian-Carnian) radiolarian fossil report (Campa *et al.*, 1982) and by the youngest detrital zircons with an age of 260 Ma (Centeno-García *et al.*, 2003); therefore, the deposition could not be older than late Permian. One sample of the sedimentary matrix of the Arteaga complex has distinctive zircon clusters at 260 Ma and 1.0 Ga, with minor clusters at 480–650 Ma and 800 Ma. The source for these peaks is most likely the Acatlán complex of the Mixteca terrane (Centeno-García *et al.*, 2011).

According to Centeno-García *et al.* (2008), deformation varies from gently folded strata to highly sheared block-in-matrix textures, and their metamorphic grade ranges up to high greenschist to amphibolite facies (Centeno-García *et al.*, 2003). Blueschist facies rocks have been reported by Talavera (2000) in the Las Ollas locality.

The undeformed 163±3 Ma Macías granite, located close to Tumbiscatio, Michoacán, cuts the deformed and metamorphosed units (Centeno-García *et al.*, 2011), which also indicates that deposition and deformation of the Arteaga complex is post-260 Ma and pre-163 Ma (Centeno-García *et al.*, 2011). The 183 Ma Tizapa metagranite of the Tejpilco metamorphic suite, with continental geochemical affinity, is considered to be the limit between the ocean floor assemblages and the continental margin (Eliás-Herrera *et al.*, 2000) and would define the exact time of accretion towards the continent. Therefore, these rocks are interpreted as a part of an Upper Triassic to Middle Jurassic subduction-related accretionary complex along the Mexican continental margin (Centeno-García, 2008).

The Arteaga sediments were deposited in a deep ocean basin, probably contemporaneously with parts of the rift-related magmatic activity (Centeno-García *et al.*, 2003; Centeno-García, 2005). The basin received deep marine, erosion-derived sediments as well as MORB-type lavas and air-fall ash deposits derived from an island arc. All this would have occurred in a marginal back arc basin or in an open ocean environment (ocean floor/continental rise setting). Deformational structures suggest that the complex was deformed during subduction processes and correspond to the upper levels of an accretionary prism (Centeno-García *et al.*, 2003).

#### *Basement cover*

Middle and Upper Jurassic to earliest Cretaceous evolved arc rhyolitic submarine lavas, volcanoclastic rocks (163–145 Ma magmatic peak; 154–157 Ma at Cuale, Jalisco, western Zihuatanejo terrane; Bissig *et al.*, 2008) and granitoids (163±3 Ma, Macías granite) cover and cross-

cut deformation and metamorphic structures, respectively. In the Early to middle Cretaceous (Barremian-Albian) arc, two magmatic peaks at 129–123 Ma and 109 Ma were identified from detrital zircons from fluvial and shallow marine rocks in the Zihuatanejo terrane (Centeno-García, 2005; Centeno-García *et al.*, 2008, 2011). This arc is considered as extensional, because detritus and zircons from the Arteaga complex, as well as from the Middle Jurassic to earliest Cretaceous and Early to middle Cretaceous arcs, were locally recycled into an Aptian-Albian intra-arc basin. Additional evidence for the existence of the arc is given by Early Cretaceous shallow marine to non-marine sedimentary formations that rest unconformably on Jurassic granitoids in the Arteaga-Tumbiscatio area (Centeno-García *et al.*, 2011). During this time span, the Late Jurassic to Early Cretaceous (Tithonian-Cenomanian) Arperos basin (Sierra de Guanajuato) was formed in a back arc regime when the Guerrero terrane drifted in the paleo-Pacific domain towards the west during extension, and was subsequently accreted back to the Mexican craton (Martini *et al.*, 2011).

The presence of recycled Santonian-Maastrichtian (85–65 Ma) arc volcanic rocks is evidenced by detrital zircons in volcanosedimentary sequences (Centeno-García *et al.*, 2011). Undeformed granitoids of Late Cretaceous and Paleogene ages are reported by Schaaf (1990), Valencia *et al.* (2009) and Martini *et al.* (2010) in the coastal Zihuatanejo terrane. This arc is interpreted by Centeno-García *et al.* (2011) as compressional, because Cenomanian strata were folded together with the Early Cretaceous strata prior to the deposition of Santonian and younger sediments, which is confirmed by an angular unconformity. Therefore, this shortening must have taken place between Turonian and Santonian (93–84 Ma).

#### *Uppermost Jurassic and Cretaceous arc successions of the study area, coastal Zihuatanejo terrane*

According to Centeno-García *et al.* (2008), the Cretaceous arc successions include basaltic, andesitic, and some rhyolitic volcanoclastic rocks, interbedded with limestones, evaporites, and red beds (Grajales-Nishimura and López-Infanzón, 1984). These successions contain abundant fossils (rudists, gastropods, microfossils, fossil logs, and vertebrates). The uppermost Cretaceous (Santonian-Maastrichtian) rocks are red beds interbedded with andesitic volcanic rocks that rest on all previously described units (Altamira-Areyán, 2002; Benammi *et al.*, 2005).

The study area is located within the Puerto Vallarta and Tepalcaltepec region with the following stratigraphy (Figure 2), based on the observations of Centeno-García *et al.* (2003) and other authors referred below.

*Jurassic limestone.* The oldest rocks in the study area are limestones found near Coquimatlán, Colima, which contain early Tithonian ammonites (150–145 Ma; Michaud *et al.*, 1987), are interbedded with volcanic and volcanoclastic rocks and are unconformably overlain by Cretaceous arc volcanic rocks.

*Alberca Formation.* The oldest Cretaceous rocks correspond to the lower Cretaceous Alberca Formation that outcrops near Colima (Pimentel, 1980). Its lower member consists of interbedded black shale, sandstone, limestone, and tuff. The upper member is composed of basaltic and andesitic flows, limestone and shale. This formation contains Berriasian-Hauterivian (145–130 Ma) ammonites (Cuevas, 1981).

*Tecalitlán Formation.* Upwards, the Alberca Formation transitionally changes to the Tecalitlán Formation (Rodríguez, 1980; Pantoja-Alor and Estrada-Barraza, 1986), which locally records the main magmatic event with andesitic, basaltic, and some minor rhyolitic flows, intercalated with pyroclastics (intermediate tuffs and ignimbrites) and lahars, reworked tuff with limolite, and calcareous sandstone. Given that it covers the Alberca Formation and is overlain by the Tepalcaltepec

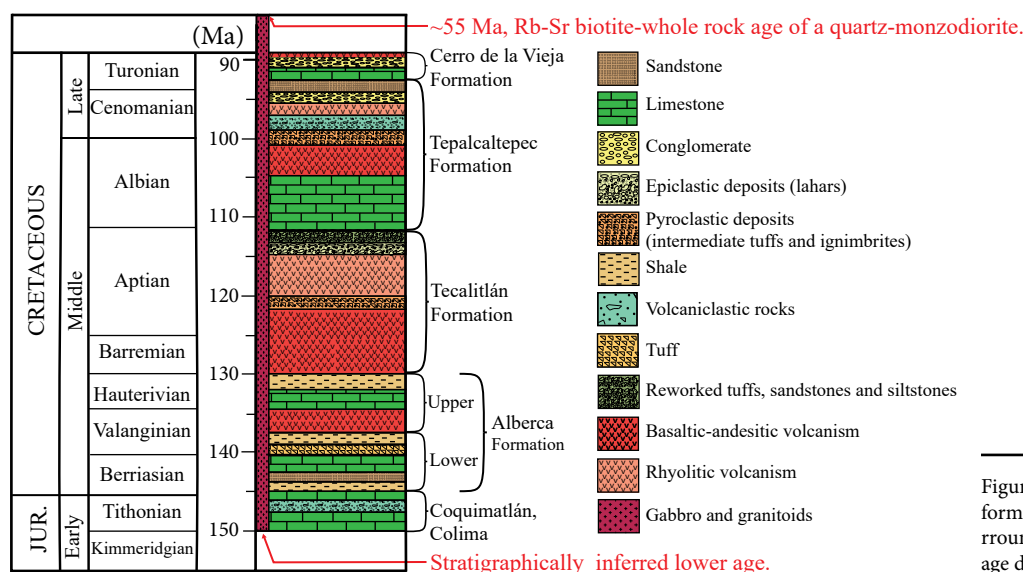


Figure 2. Stratigraphic column with the main formations in the study area and its close surroundings. Rb-Sr biotite-whole rock cooling age determined by Schaaf (1990).

Formation, a Barremian-Aptian age (130–112 Ma) is presumed. Additionally, near La Minita, in the Pihuamo region, the Tecalitlán Formation contains early Aptian rudists (125 Ma; Centeno-García *et al.*, 2011 and references therein). A 118.5±2.5 Ma K-Ar hornblende age was reported for a porphyritic andesite, collected west of Tepalcaltepec, that is considered as the upper part of Tecalitlán Formation (Bermúdez-Santana, 1994).

**Tepalcaltepec Formation.** Apparently, the volcanic activity decreased during the early Albian and finally ceased in the middle to late Albian. During this time span, the Tepalcaltepec Formation was deposited (Pimentel, 1980), composed of thick limestone layers intercalated with andesitic flows and some rhythmic volcanoclastic and calcareous deposits, tuffs and rhyolites, conglomerates and sandstones, red limolites, and some evaporites (Grajales-Nishimura and López-Infanzón, 1984). A reef-type limestone with a fossil record indicating an Albian-Cenomanian age (112–93 Ma) was reported by Corona (1999). In the central Colima region, the Tepalcaltepec Formation laterally changes to the Madrid Formation (Pano, 1975), which consists of thin-bedded limestone, calcareous shale, gypsum, and few andesitic flows and tuff. The studied fossils are of Albian to early Cenomanian age (112–99 Ma, Grajales-Nishimura and López-Infanzón, 1984). According to Centeno-García *et al.* (2011), the Madrid and Tepalcaltepec formations may correlate with the Encino (late Aptian fossils, Buitrón, 1986) and Vallecitos (early Albian fossils, Alencaster, 1986) formations, respectively (both ~112 Ma). The contact between the Tecalitlán and Tepalcaltepec formations could not be established in this study; however, Centeno-García *et al.* (2011) stated that the Tecalitlán Formation was tilted prior to the deposition of the Encino Formation. We assume the same type of contact between the Tecalitlán and Tepalcaltepec formations in the study area.

**Cerro de la Vieja Formation.** The Cerro de la Vieja Formation (Parga, 1977) constitutes a conglomeratic unit composed of limestone fragments, which was folded together with the underlying Cenomanian limestone. Interlayered lava flows were dated by the K-Ar method at 80±6 and 78±6 Ma (Grajales-Nishimura and López-Infanzón, 1984). Conglomerates contain sandstone and silt layers with sedimentary structures and textures that suggest a fluvial continental depositional environment.

**Granitoids and gabbros.** Some of the formations listed above are

intruded by granitoids with ages between 68 and 55 Ma (four K-Ar biotite and hornblende ages, three Rb-Sr biotite-whole rock ages, as well as an eight point whole rock isochron; Schaaf, 1990). As observed in the field, most of these granitoids also intrude gabbroic intrusive rocks in the study area.

### GEOCHEMISTRY OF THE EARLY CRETACEOUS ARC – PREVIOUS WORKS

Most geochemical studies in the area were focused on the Early Cretaceous volcanic rocks (*e.g.*, Centeno-García *et al.*, 2011). Rocks of the continuous chain of plutons along the Mexican Pacific margin range from gabbros, plagiogranites, quartz monzodiorites to tonalites and from granodiorites to granites. The plutonic rocks with the highest silica and potassic feldspar content occur in the Puerto Vallarta batholith, whereas plagiogranites (M-type granites; Pitcher, 1982) and gabbros have only been observed so far between Manzanillo and Jilotlán (Schaaf, 1990; Schaaf *et al.*, 1995).

Geochemical, isotopic, and geochronological studies on the intrusive rocks of the Mexican Pacific coast between Puerto Vallarta and Acapulco reported by Schaaf (1990), Schaaf *et al.* (1995, 2000), and Morán-Zenteno *et al.* (2000) show SiO<sub>2</sub> variations between 47.3 and 76.9 wt. %, calc-alkaline character, as well as volcanic arc affinities deduced from Rb vs Yb+Nb diagrams. The alumina saturation index (molar Al<sub>2</sub>O<sub>3</sub>/Na<sub>2</sub>O+K<sub>2</sub>O+CaO) is, in general, lower than 1.1, which corresponds to I-type granites (Pitcher, 1982). These Mesozoic-Cenozoic intrusive show heterogeneous initial <sup>87</sup>Sr/<sup>86</sup>Sr from 0.7033 to 0.713 and εNd values between +6.4 and -7. The most radiogenic Sr and least radiogenic Nd isotopic ratios are from the eastern portion of the Puerto Vallarta batholith, whereas the magmatically most primitive values are found between Manzanillo, Jilotlán, and Petatlán-Papanao in the Colima, Jalisco, and Guerrero states, respectively. For plagiogranites intruding the Jilotlán gabbros a crystallization age of 68±12 Ma was obtained from a low-radiogenic eight point whole rock Rb-Sr isochron with an initial <sup>87</sup>Sr/<sup>86</sup>Sr of 0.70377. The initial εNd values for the granitoids are between +3.5 and +4.3 and for a gabbro sample a +7 value was obtained (Schaaf, 1990). Gabbros have been also reported from the Manzanillo pluton and further to the NW along roadcuts

between Barra de Navidad and La Huerta, Jalisco, which form a  $69 \pm 3$  Ma 14-point Rb-Sr isochron (Schaaf, 1990, 2002). This age is similar to the  $67 \pm 1$  Ma U-Pb zircon age obtained from the Compuertas mafic intrusive near Manzanillo (Panseri, 2007). Delgado-Argote *et al.* (1992) studied diorites, gabbros and ultramafic rocks (dunite-clinopyroxenite) in Petatlán-Papanao and El Tamarindo, southeast of Zihuatanejo, Guerrero. They published a  $\sim 112$  Ma  $^{40}\text{Ar}/^{39}\text{Ar}$  hornblende age for an ultramafic body. Recently, Ferrari *et al.* (2014) reported U-Pb zircon ages of  $47.9 \pm 1.8$  Ma and  $41.3 \pm 0.6$  Ma, and one  $^{40}\text{Ar}/^{39}\text{Ar}$  feldspar age of  $36.1 \pm 0.5$  Ma for gabbros from the Petatlán-Tecpan area.

The volcanic rocks of the Guerrero terrane range from basalts, andesites and dacites to rhyolites, with Th/Yb and Ta/Yb ratios indicating transitions between oceanic island arcs and continental margin arcs (Centeno-García *et al.*, 1993, 2003; Tardy *et al.*, 1994; Freydier *et al.*, 1997; Mendoza and Suástegui, 2000). The basalts have REE patterns similar to those of island arc rocks, with negative Eu anomalies (Centeno-García *et al.*, 1993; Freydier *et al.*, 1997). Felsic lavas are calc-alkaline and show LREE enrichment compared to the basalts (Freydier *et al.*, 1997). The initial  $\epsilon\text{Nd}$  parameters are between +3 and +7.8 for all compositions (Centeno-García *et al.*, 1993; Freydier *et al.*, 1997), similar to modern island arcs. Neodymium  $T_{\text{DM}}$  model ages span from 290 to 460 Ma, which excludes the participation of Precambrian crust in magma generation processes (Centeno-García *et al.*, 1993).

## GEOLOGY AND FIELD WORK

Figure 3 shows the geological map of the study area elaborated from fieldwork observations and photointerpretation. The Jilotlán pluton is composed by granitoids of tonalitic to granodioritic compositions that intrude a gabbroic body. The gabbros are located in the central part of the pluton between Jilotlán and Tecalitlán.

The granitoids intrude the Tecalitlán Formation, which is the host rock. Locally, outcrops of this formation are highly altered. Lavas of the Tecalitlán Formation are primarily andesitic in composition and in less proportion dacitic. Few fine-grained sandstone layers alternate with the lavas. The overall formation is highly fractured and faulted (Figure 4a).

The gabbros and the granitoids exhibit textural variations. Gabbros almost always occur as microgabbros with some subordinate coarse-grained species (Figure 4b). The gabbros were cool when they were intruded by the granitoids, which is indicated by sharp contacts.

Within the granitoids, an alignment of mafic enclaves was observed (Figure 4c, 4d), as well as potassium feldspar crystals in contact with pyroxenes, characteristic for a mineral association in disequilibrium (not shown). Cumulates of hornblende and pyroxenes are also present. All this suggests that mingling involving mafic and felsic minerals occurred within the felsic facies of the pluton, probably produced by fractional crystallization of a parental mafic magma.

Pegmatites within the pluton contain plagioclase pheno- and

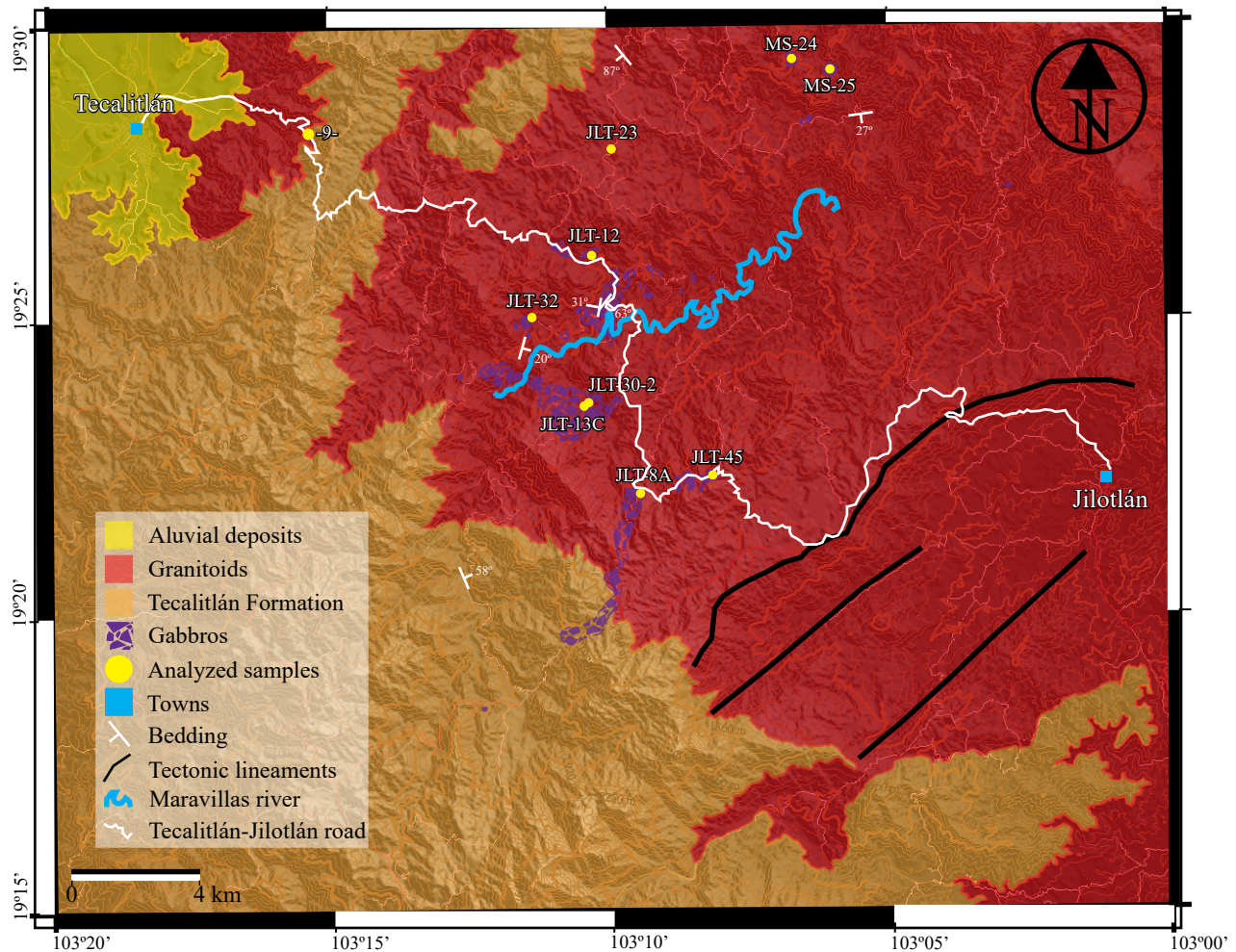


Figure 3. Geologic map of the study area and location of the analyzed samples. The topographic map E13B46 from INEGI (scale 1:50,000) was used as base.

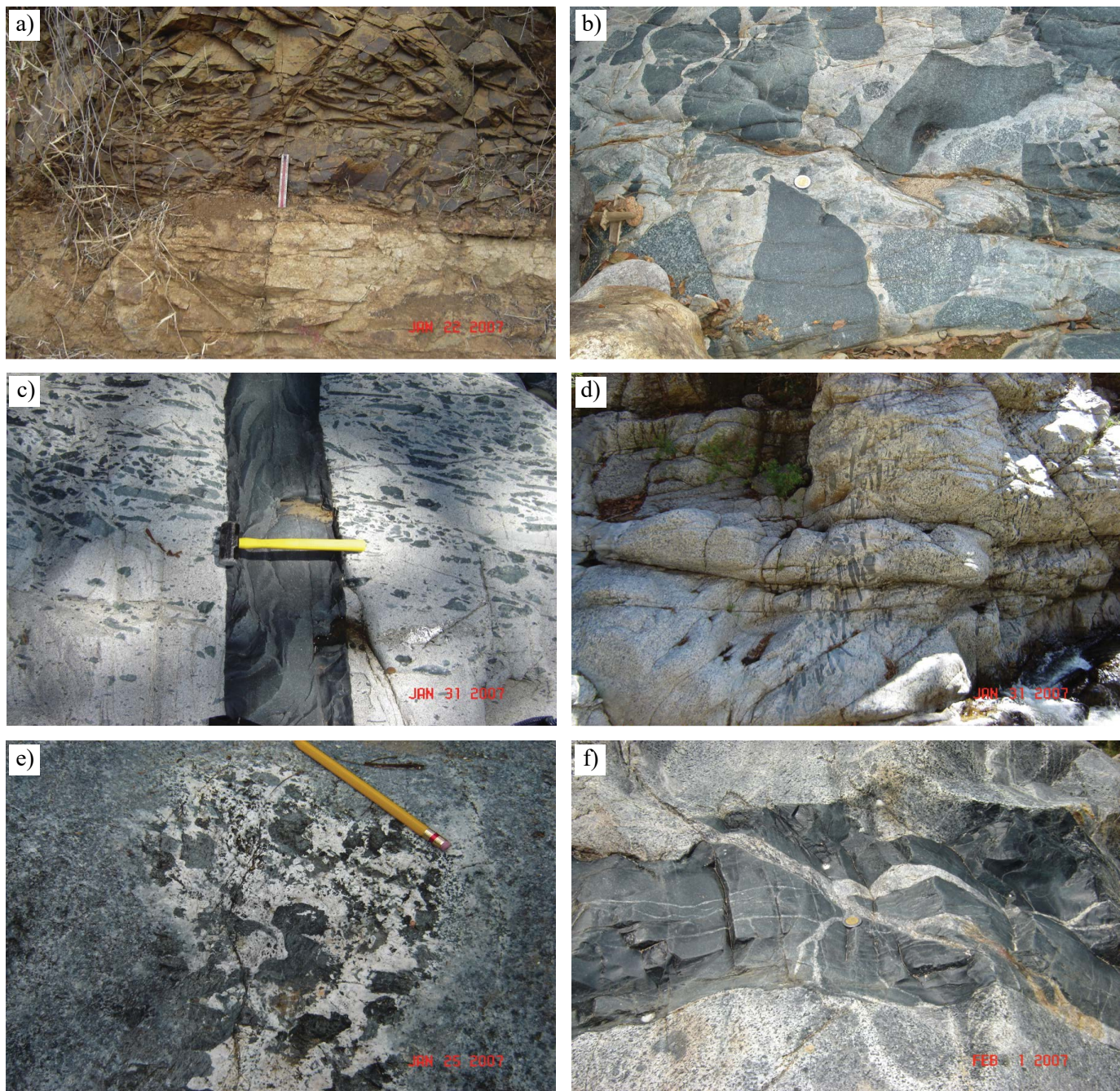


Figure 4. a) Contact of the Tecalitlán Formation with a granitic body/dike. b) Microgabbros and coarse grained gabbros intruded by a tonalitic to granodioritic body. c) Mafic porphyritic dike intruding a tonalitic to granodioritic body with mafic enclaves. d) Syntectonic alignment of mafic enclaves in the felsic body. e) Pegmatite with amphibole and pyroxene phenocrysts in a gabbro with potassic feldspar and pyroxenes. f) Several generations of dikes intruding a tonalitic body of the Jilotlán pluton.

megacrysts, amphibole, and some pyroxenes in the gabbroic parts (Figure 4e). In the more felsic areas, phenocrysts and megacrysts of quartz and potassium feldspar were observed; some parts of the felsic bodies display aplitic textures.

Several generations of mafic dikes (Figure 4c, 4f) with aphanitic-porphyrific to aplitic phaneritic-porphyrific textures intrude all facies of the Jilotlán pluton as well as the Tecalitlán Formation (Figure 4c, 4d, and 4f). The dikes show a preferred NE-SW orientation and a thickness ranging from a few centimeters up to five meters.

In the Tepalcaltepec area, outcrops of granodiorite, gabbro, and

mafic dikes were observed. A thick ignimbrite layer covers the gabbros. Further to the west, conglomerates overlie packages of fossil-rich limestone, intercalated with sandstone and shale. At La Codiciada mine (Figure 1a) the intrusion event formed a skarn with barite and wollastonite mineralization.

Samples of the gabbros and granitoids, as well as host rocks and mafic and felsic dikes of the Jilotlán-Tecalitlán area were collected. One gabbro from Tepalcaltepec was also sampled. Additionally, two gabbro samples were obtained from the Manzanillo batholith on the Solidaridad viewpoint over Bahía de Santiago along the

Manzanillo-Cihuatlán bypass road, approximately 4 kilometers NW from Manzanillo. The Manzanillo gabbros show considerable textural variations in distances of just a few meters apart, expressed by very fine to coarse-grained zones with magmatic foliations, and pyroxene and hornblende cumulates. All sampling locations are shown in Figures 1a and 3.

**PETROGRAPHY**

Detailed petrographic descriptions were performed on the most important units between Tecalitlán and Jilotlán. Five gabbros were selected (JLT-8A, JLT-12, JLT-30-2, JLT-32 and JLT-45), as well as one granitoid (quartz-monzodiorite JLT-23), one host rock sample (-9-), and one mafic dike (JLT-13C). Additionally, one gabbro sample from Tepalcaltepec (JLT-41) and two gabbros from Manzanillo (MZ-3, MZ-4) were analyzed.

The point counting results and corresponding classification names are given in Table 1 (except for host rock -9-). Microphotographs showing petrographic features of the samples are included as Figures A1 to A5 of the Supplementary Material.

In general, gabbroic samples present equigranular textures. Euhedral and/or anhedral plagioclase crystals, the most abundant mineral (Figure A1), have anorthite contents of 60 to 68% determined

by the Michel-Levy method. Some crystals show antiperthitic textures (Figure A1b), evidencing lack of mixture in the rock, and saussuritization, which implies a compositional change from calcic to sodic plagioclase (e.g., Figure A1d; quartz-monzodiorite). Some plagioclase crystals are also sericitized.

The second most abundant mineral is black and green hornblende that is frequently chloritized. In many cases, it is not distinguishable from clinopyroxene due to alteration and uralitization (Figure A2a). Poikilitic textures were observed in hornblende oikocrystals containing plagioclase, pyroxene and oxides (Figure A2b, A2c). Some gabbros present biotitization of hornblende and/or pyroxene (Figure A2d). Besides chlorite, epidote is another abundant alteration mineral in hornblende, probably due to hydrothermal or meteoric alteration (Figures A1a, A3a, A3b, A3c). Several clinopyroxene and pseudomorphic hornblende crystals show plagioclase inclusions (Figure A3d). This, together with the pyroxene crystals surrounded by hornblende, could indicate an excess of calcium content during hydration of the magmatic system, leaving calcium to crystallize as plagioclase. On the other hand, rapid magma ascent could have generated a lack of mixture between clinopyroxene and plagioclase in the magmatic system.

Oxides display a skeletal texture and most of them are surrounded by titanite, (Ti-rich magnetite, Figures A1b, A2e, A3e). This texture results when hornblende and pyroxene require iron for formation, leaving the excess titanium to crystallize around the corroded oxides.

Table 1. Point counting results and modal classification of the analyzed samples.

Sample	JLT-8A	JLT-12	JLT-13C	JLT-23	JLT-30-2	JLT-32	JLT-41	JLT-45	MZ-3	MZ-4
Plagioclase (P)	388	401	268	378	339	381	284	380	422	449
Hornblende	133	265	226	42	223	223	262	202	49	283
Clinopyroxene	4	12	3	14	0	3	0	0	81	2
Orthopyroxene	0	13	0	0	0	0	0	0	0	0
Biotite	29	0	0	28	0	1	0	5	0	3
Alkali Feldspar (FK)	3	44	0	91	0	3	0	0	0	0
Quartz (Q)	0	0	0	59	0	0	0	0	0	0
Oxide	31	18	-	10	14	86	26	35	35	33
Titanite	19	0	0	0	24	0	0	9	0	0
Chlorite	8	6	10	8	17	-	11	-	0	1
Epidote	5	0	1	0	2	5	1	-	0	4
Sericite	0	6	8	0	0	-	-	0	0	0
Calcite	0	4	0	7	0	8	3	0	0	2
Total	620	769	516	637	619	710	587	631	587	777
P+Q+FK	391	445	268	528	339	384	284	380	422	449
P (%)	99.23	90.11	100	71.59	100	99.2	100	100	100	100
Q (%)	0	0	0	11.17	0	0	0	0	0	0
FK (%)	0.76	9.88	0	17.23	0	0.78	0	0	0	0
Total (%)	99.99	99.99	100	99.99	100	99.98	100	100	100	100
Classification	Middle-grained hornblende, biotite and clinopyroxene microgabbro.	Middle-grained hornblende, orthopyroxene and clinopyroxene microgabbro.	Aphanitic basaltic dike with xenoliths.	Middle-grained hornblende, biotite and clinopyroxene quartz-monzodiorite.	Fine-grained hornblende microgabbro.	Middle-grained hornblende, clinopyroxene and biotite microgabbro.	Middle-grained hornblende and clinopyroxene microgabbro.	Fine-grained hornblende and biotite microgabbro.	Fine-grained clinopyroxene and hornblende microgabbro.	Middle-grained hornblende, biotite and clinopyroxene gabbro.

Plagioclase (P), potassium feldspar (FK) and quartz (Q) points normalized to 100% and reported in % units were used for the modal classification in the Streckeisen (1979) diagram (not shown). Rocks were considered microgabbros when the plagioclase size was fine- (< 1mm) to medium-grained (1 to 5 mm). The size of the mafic minerals was also determined, and is mentioned in each classification. A (-) mark appears when a mineral was altering another mineral, for example, chloritized hornblende was counted as hornblende. All opaque minerals were considered as oxides, and few samples presented sulphides in the field or in hand sample.

Prehnite and potassium feldspar were observed in a few samples (Figure A3e) evidencing metasomatism related to the granitoid intrusion. The reason for the absence of potassium feldspar in some samples may lie on a local lack of fluids to achieve homogeneous potassium oversaturation or due to a sampling bias.

The basaltic dike (JLT-13C) contains mafic xenoliths with clinopyroxene, hornblende, prehnite and epidote crystals (Figure A4a, A4b). There are also mafic crystals, including actinolite, that form a cumulophyric texture (Figure A4c, A4d).

The quartz-monzodiorite (JLT-23, Figures A1c, A4e, A4f, A5a) contains plagioclase ( $An_{52}$ ), hornblende, biotite, and accessory clinopyroxene and titanite. The host rock sample from the Tecalitlán Formation (-9-, Figures A5b, A5c, A5d, A5e), collected near the contact with the granitoid, was petrographically analyzed but not point counted because many parts of the thin section are highly altered and the minerals could not be distinguished. Due to the presence of andalusite, white mica, rounded quartz and plagioclase, the rock is classified as quartz-rich sandstone metamorphosed during the granitic intrusion.

## GEOCHEMISTRY

### Major elements

Major elements were obtained by X ray fluorescence at the Laboratorio Universitario de Geoquímica Isotópica (LUGIS), Instituto de Geología, Universidad Nacional Autónoma de México (UNAM). All analytical procedures can be consulted in Lozano Santa-Cruz and Bernal (2005) and Villanueva-Lascurain (2011). Concentrations are expressed as weight percentage and iron is expressed as total  $Fe_2O_3$ . For the AFM diagram  $Fe_2O_3$  and FeO were automatically calculated with the Petrograph software (Petrelli *et al.*, 2005) and also manually calculated using  $Fe_2O_3 = Fe_2O_3 \times 0.15$  and  $FeO = Fe_2O_3 \times 0.85 \times 0.8998$  (Ragland, 1989).

Table A1 of the Supplementary Material presents the analytical results of the 10 samples described petrographically (except the host rock) together with their coordinates and altitudes. Additionally, two gabbros from Jilotlán (MS-24 and MS-25) from Schaaf (1990), a gabbro from Aquila (Aq-1), a meta-sandstone near Tecalitlán (ATG-1) and two Rivera plate basalts (D5-2Ext and D5-2Int) from Valdez-Moreno (2006) were used for comparison.

Most gabbros and the quartz-monzodiorite from Jilotlán are sub-alkaline according to the silica vs. total alkalis diagram (Figure 5a) of Cox *et al.* (1979), although some samples plot on the dividing line. In the silica vs. potassium diagram of Peccerrillo and Taylor (1976) (Figure 5b), the majority of Jilotlán (JLT, MS), Aquila (Aq-1) and Manzanillo (MZ) gabbros form part of the middle potassium calc-alkaline series. The quartz-monzodiorite (JLT-23) and the Tepalcaltepec gabbro (JLT-41) are more enriched in potassium, whereas the JLT-30-2 gabbro from Jilotlán is shoshonitic. Gabbro MS-24, the basaltic dike JLT-13, and the Rivera basalt samples (D5-2) are tholeiitic.

Sodium enrichment in basalts has been explained by hydrothermal alteration, and high potassium content in granites can be the product of contact metamorphism (Rollinson, 1993). These anomalies are probably due both to hydrothermal alteration and metasomatism caused by the intrusion of the granites. This explains the crystallization of potassium feldspar present in some gabbros (*e.g.*, Figure A3e) by metasomatic potassium oversaturation.

### Trace elements

Trace element concentrations of Jilotlán, Tepalcaltepec, and Manzanillo samples (Table A2 of the Supplementary Material) as well as those from Aquila and the Rivera plate reported by Valdez-Moreno (2006) were obtained by ICP-MS at the Laboratorio de Estudios Isotópicos (LEI), Juriquilla, UNAM (methods described in Mori *et al.*, 2007; Villanueva, 2011). Sample MS-25 was analyzed by neutron activation analysis at the University of Mainz, Germany (Schaaf, 1990).

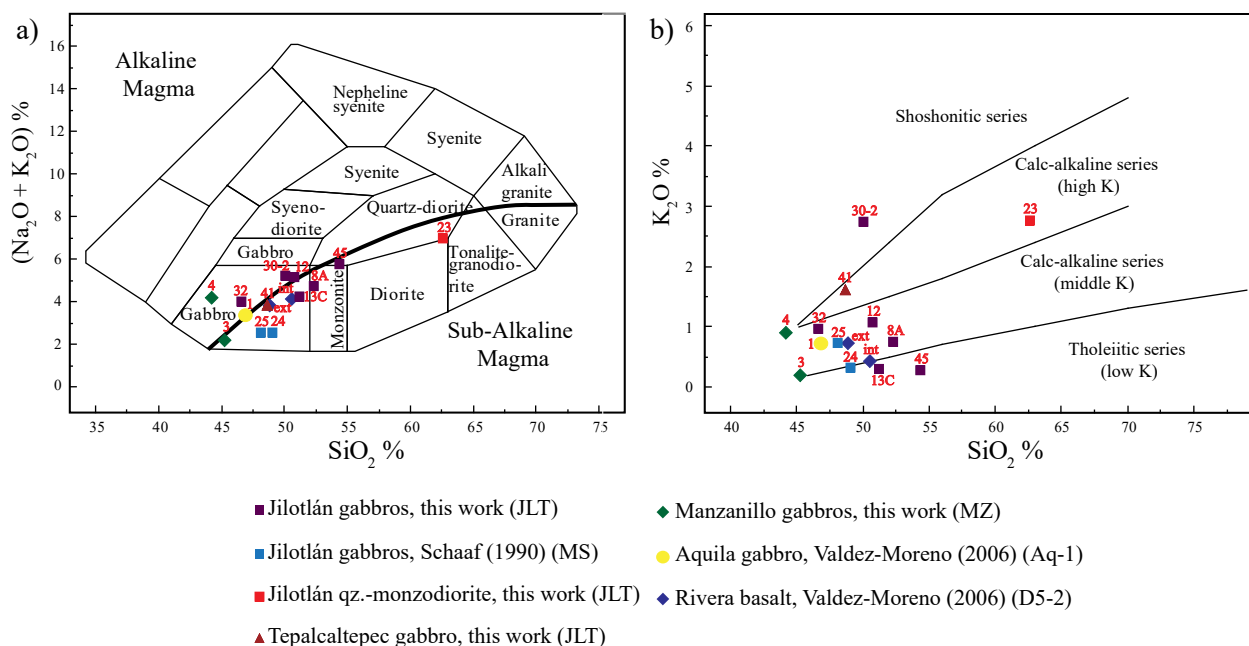


Figure 5. a) Classification diagram of silica ( $SiO_2$ ) versus total alkalis ( $Na_2O + K_2O$ ) for plutonic rocks, modified from Cox *et al.* (1979). b) Silica ( $SiO_2$ ) versus potassium ( $K_2O$ ) subclassification diagram for subalkaline plutonic rocks of Peccerrillo and Taylor (1976). Sample numbers are given above each symbol (see Table 2). Two gabbros from Jilotlán (MS-24 and MS-25) from Schaaf (1990) as well as a gabbro from Aquila (Aq-1) and two Rivera plate basalts (D5-2Ext and D5-2Int) from Valdez-Moreno (2006) are included for comparison.

The trace element behavior in the investigated gabbros and the quartz monzodiorite is shown in a multielement diagram (Figure 6, normalized to N-MORB of Sun and McDonough, 1989). Nearly all rocks show enrichments in the most incompatible elements but have similar values in the less incompatible ones compared to N-MORB and to the Rivera plate sample (D5-2int). However, D5-2int also shows enrichments in the most incompatible elements (e.g., Cs, Ba) when compared to N-MORB, possibly due to secondary alteration processes.

The gabbro from Jilotlán with the lowest overall element concentrations is JLT-32 (except for Cs, Rb and Ba) suggesting its origin from an even more depleted source; the one with the highest concentrations (except for the most incompatible elements) is JLT-30-2, being also the only sample without positive Sr and Pb spikes in Figure 6. This is probably due to the fact that plagioclase is not calcic enough to concentrate Sr, and most Pb was removed by hydrothermal alteration. Sr is abundant in carbonate phases, concentrates in calcic plagioclase, and can be transported in aqueous solutions (e.g., derived from calcareous sediments in the subducted slab). Pb is also transported in aqueous solutions derived from marine or continental sediments of the subducted slab or the continental crust. This explains the positive Sr and Pb anomalies in most Jilotlán gabbros compared to the Rivera plate basalts (Figure 6). The negative Nb anomaly is apparently due to fractionation of ilmenite and/or rutile, given that hornblende and titanite are widely present in the gabbros.

The Tepalcaltepec (JLT-41), Aquila (Aq-1), and Manzanillo (MZ-3, MZ-4) gabbros show similar trace element patterns in comparison to those from Jilotlán, with higher Rb and Ba values for JLT-41, possibly caused by metasomatic processes. The Aquila gabbro (Aq-1) shows slightly lower concentrations in most trace elements than those of Jilotlán, indicating a more depleted source. However, high positive Sr and Pb anomalies suggest greater plagioclase accumulation and crustal participation, respectively, in comparison to Jilotlán. The Manzanillo gabbro MZ-3 reveals the lowest trace element concentrations of all studied samples, except for Sr. This is probably due to a very high Ca content in plagioclase (58% An). The source of this rock is more depleted than that of Jilotlán, Tepalcaltepec and Aquila. Interestingly, the MZ-4 sample, collected just a few meters away from MZ-3, shows

the mean trace element concentrations for Jilotlán, Tepalcaltepec and Aquila.

The quartz-monzodiorite (JLT-23) has higher Cs, Rb, Ba, Th and U values in comparison to the gabbros, which indicates that its source is more enriched. Well-defined positive Sr and Pb anomalies are best explained by calcic plagioclase accumulation (52% An) and a sediment component, respectively, which is also supported by high Th and U values. Less incompatible elements such as Dy, Ho, Er, Yb, and Lu have lower values than in the gabbros, suggesting a slightly more evolved magmatic source.

The meta-sandstone (ATG-1) has overall patterns and concentrations comparable to the JLT-23 quartz-monzodiorite. The negative Ba anomaly could be caused by potassic feldspar removal, and the high Th and U values indicate a continental source, also comparable to JLT-23. The Pb contents are the highest and Sr and Eu the lowest of all samples, which emphasizes the origin from a continental source and plagioclase erosion, respectively.

REE patterns

The Rare Earth Element (REE) patterns (normalized to the CI Carbonaceous Ivuna chondrite values of McDonough and Sun, 1995) of all samples displayed in Figure 6 are graphed in Figure 7. All show negative slopes (with the exception of the Rivera plate basalt D5-2int), which result from the enrichment in light REE (LREE) with respect to the heavy REE (HREE). Two groups are distinguishable within the Jilotlán gabbros: samples JLT-30-2, JLT-45, JLT-8A and JLT-13 with stronger LREE enrichment in comparison to samples JLT-32, JLT-12 and MS-25. The Tepalcaltepec gabbro JLT-41 shows very similar REE patterns to the Jilotlán gabbros, whereas the Aquila sample (Aq-1) has lower concentrations. The Manzanillo MZ-3 sample displays a positive Eu anomaly, probably because reducing conditions with overall low oxygen fugacity caused  $\text{Eu}^{+2}$  substitution for Ca in accumulated plagioclase. On the other hand, the MZ-4 gabbro shows a slight negative Eu anomaly, which suggests that  $\text{Eu}^{+2}$  was captured by Ca-rich plagioclase during fractionation. Therefore, the opposite Eu anomaly behavior of both MZ samples suggests different processes involved in the generation of the Manzanillo gabbros from the same source, which could have been even more depleted than the sources of the Jilotlán,

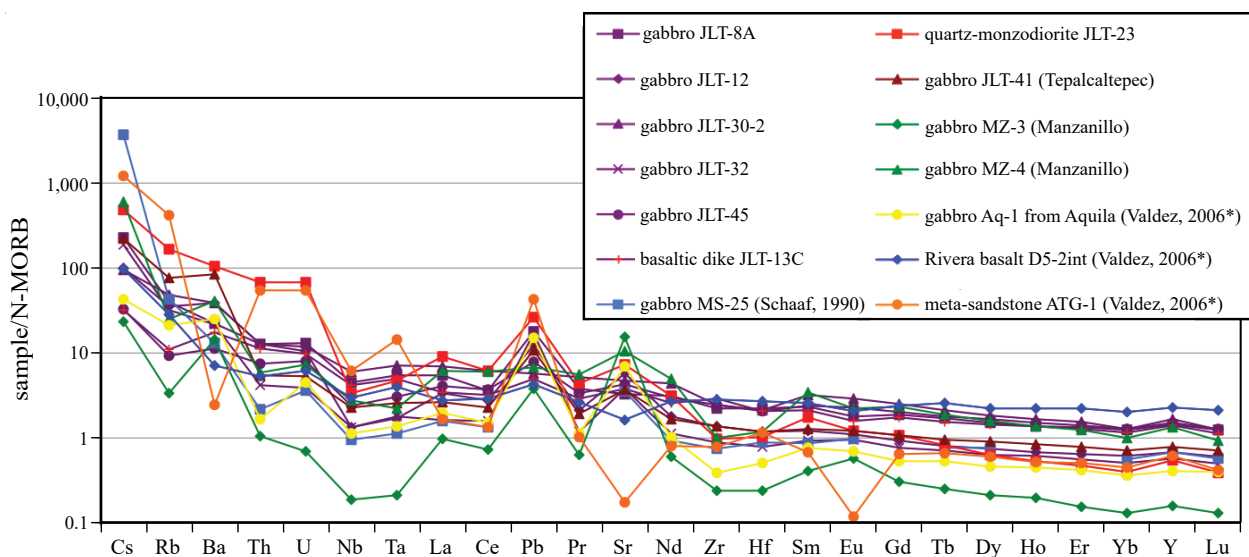


Figure 6. Multielemental diagram normalized to N-MORB (Sun and McDonough, 1989) with increasing compatibility from left to right for the analyzed rocks of this and previous studies. \*Valdez-Moreno (2006).

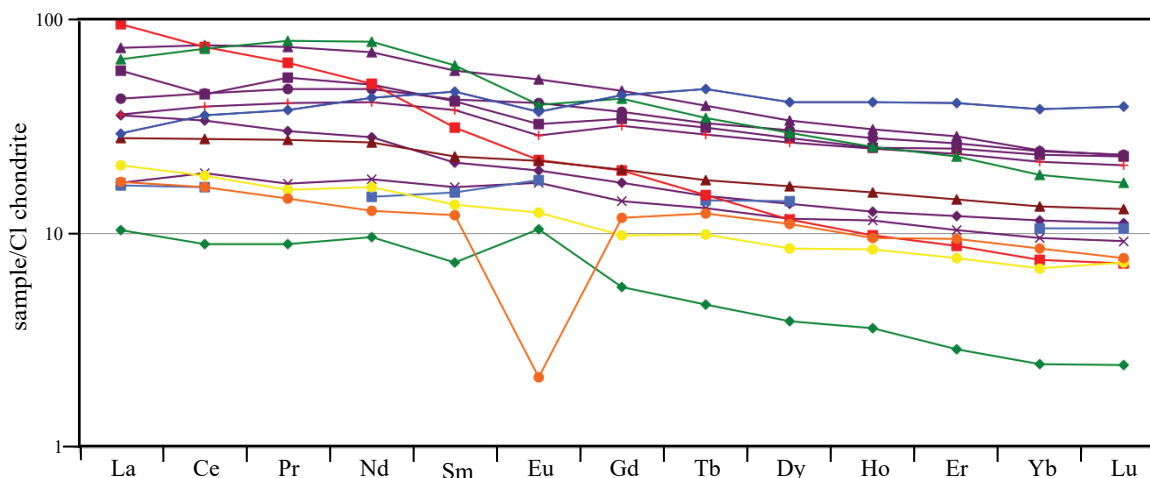


Figure 7. REE distribution patterns normalized to CI chondrite values of McDonough and Sun (1995) with increasing compatibility from left to right in the analyzed rocks of this and previous studies (see legend in Figure 6).

Tepalcaltepec and Aquila gabbros. Sample MZ-3 represents also the most depleted gabbro of all according to REEs.

The JLT-23 quartz-monzodiorite crosscuts both groups of Jilotlán gabbros with stronger LREE/HREE fractionation. This suggests that it originated from a more evolved source than the gabbros.

The meta-sandstone ATG-1 has generally very low REE concentrations and a pronounced negative Eu anomaly probably due to the absence of Ca-rich plagioclase.

Jilotlán, Tepalcaltepec (JLT), Aquila (Aq-1) and Manzanillo (MZ) gabbros have trace element distribution patterns (Figure 6) with typical subduction zone geochemical signatures such as high Large Ion Lithophile Element (LILE) concentrations in comparison to High Field Strength Elements (HFSE) and REE, as well as positive Pb and Sr anomalies. These signatures could be attributed to fluid release from the subducted slab/sediments to the mantle wedge (Plank and Langmuir, 1998; Winter, 2001). Rare earth element patterns (Figure 7) are LREE enriched compared to HREE, which can be accomplished by low degrees of partial melting or high degrees of fractional crystallization from a primitive mantle source (e.g., Winter, 2001). The relatively flat pattern in HREE rules out a garnet presence in the source.

#### Tectonomagmatic environment

To crosscheck the magmatic environment in which the Jilotlán gabbros were generated, we selected the triangular Zr/4-2Nb-Y diagram for basalts of Meschede (1986) (Figure 8). Although this diagram was constructed on the basis of 1800 basalt analyses, it can be used also for gabbros like those from this study. Most of the Jilotlán and the Tepalcaltepec samples, with the exception of MS-25, situate in the C field that corresponds to intra-plate tholeiites and volcanic arc basalts. Gabbro MS-25 together with those from Aquila (Aq-1) and Manzanillo (MZ), as well as the Rivera plate basalt (D5-2int), plot in the D field that corresponds to normal mid ocean ridge basalts (N-MORB) as well as volcanic arc basalts. The JLT-23 quartz-monzodiorite plots in the volcanic arc granite (VAG) field in the Rb vs Yb+Ta diagram of Pearce *et al.* (1984; not shown) for granitic rocks.

#### Models for magmatic processes

To understand which processes generated the geochemical differences between the Jilotlán gabbros and the other igneous rocks, REEs were used in partial melting and fractional crystallization models from a hypothetical source. We chose the batch melting model of

Shaw (1970) (Equation 1), in which the melt is in equilibrium with the solid up to a critical amount and separates from the solid as an independent system. This simple model explains best the trace element distributions of MORB, the most adequate material to study mantle melting. The Rayleigh crystal fractionation model (Equation 2) is a continuous crystallization model in a closed reservoir in which each crystal is separated from the melt as soon as it forms; therefore there is no equilibrium between the solid and the melt. Equations for both models are shown below:

$$\frac{C_i}{C_i^0} = \frac{1}{\bar{D}_i(1-F) + F} \quad (1)$$

$$\frac{C_i}{C_i^0} = (1-X)^{(\bar{D}_i-1)} \quad (2)$$

where  $\bar{D}_i$  is the global partition coefficient;  $C_i$  is the trace element concentration in the source rock;  $C_i^0$  is the trace element concentration in the melt;  $F$  is the partial melting percentage of the rock; and  $X$  is the percentage of crystals removed. Concentrations can be given in ppm or wt.%.

Both equations were solved for  $C_i$ . From the partition coefficients ( $D_i^A$ ) of trace elements for different minerals in a magma with a given composition, the global partition coefficients were obtained ( $\bar{D}_i$ ) resolving  $\bar{D}_i = \sum W_A D_i^A$  where  $W_A$  is the weight fraction of mineral  $A$  in the rock and ( $D_i^A$ ) is the partition coefficient of element  $i$  in mineral  $A$ .  $C_i$  was chosen from determined data of a real rock that is the hypothetical source rock.

Given that a probable source for the gabbros is a garnet-free mantle, an upper mantle plagioclase peridotite was considered as the source material. The theoretical source rock was composed of 53% olivine, 28% orthopyroxene, 17% clinopyroxene, and 2% plagioclase (after Gómez-Tuena *et al.*, 2007). The initial concentrations ( $C_i$ ) in ppm were La=0.192, Ce=0.550, Nd=0.581, Sm=0.239, Eu=0.096, Dy=0.505, Er=0.348, Yb=0.365, and Lu=0.058 according to the values of the average depleted mantle of Workman and Hart (2005). These values were taken mostly from White (2005) and some elements in olivine and Lu in plagioclase from Winter (2001) (Table A3 of the Supplementary Material).

Only the concentration of the elements in the melt ( $C_i$ ) was calculated, as all samples plot between the batch melting and crystallization curves obtained in Nb/Zr vs. Nb and La/Sm vs. La

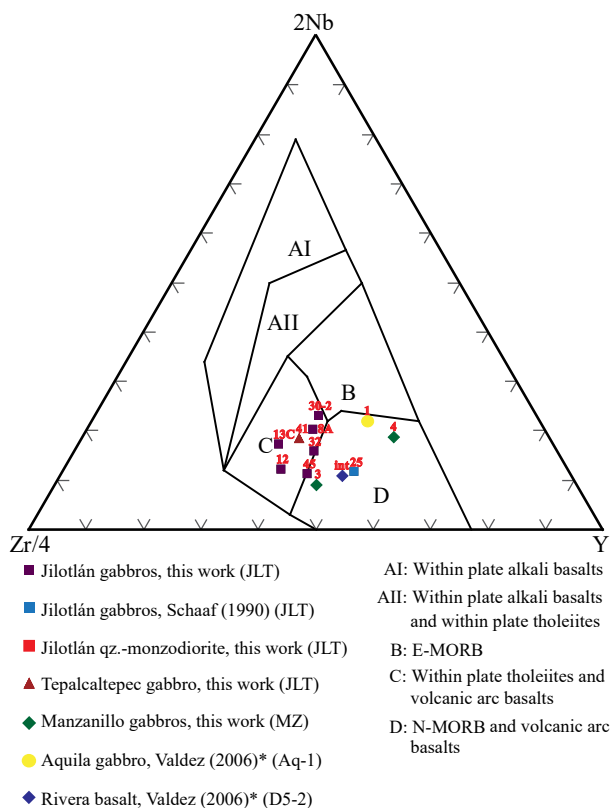


Figure 8. Discrimination diagram for the tectonic setting of basalts (Zr/4-2Nb-Y) of Meschede (1986). Sample numbers are given above their symbols (see Table 2). \*Valdez-Moreno (2006).

diagrams (not shown here) and none of them even close to the residue curves (Villanueva, 2011). On the basis of the chemical similarities observed in the previous diagrams, the Jilotlán samples were graphed separately (Figures 9a and 9b).

For a melt, small degrees of melting ( $F$ ) or high degrees of crystallization ( $X$ ) will greatly increase the content of the most incompatible LREE but will not significantly affect the least incompatible HREE. On the other hand, high degrees of  $F$  or low degrees of  $X$  will greatly decrease the content of the least incompatible HREE and will leave the most incompatible LREE unaffected. Between 1 and 99%, 1% increments were tested for both  $F$  and  $X$  to see which values best reproduce the patterns displayed by all samples. None of the obtained curves fully reproduces these patterns; however, low degrees of  $F$  and high degrees of  $X$  give the closest approximation.

As to the quartz-monzodiorite (JLT-23), 1% melting of the depleted average mantle partially reproduces its pattern; although the REE concentrations of the sample are slightly higher (Figure 9a). In the case of gabbros, the enriched set (JLT-30-2, 45, 8A and 13C) can be approximately matched by 97 to 99% crystallization from the complete melting of this mantle, whereas the more depleted set (JLT-12, 32 and MS-25) agrees with 94 to 97% crystallization of the complete mantle melt. The Tepalcaltepec gabbro (JLT-41) is partially reproduced by 96 to 97% melt crystallization (Figure 9b) and for the MZ-4 gabbro a melt crystallization of 98 to 99% best models its REE pattern and concentrations. As for MZ-3 gabbro, a 3 to 20% mantle melting would partially reflect the obtained patterns. In the case of the Aq-1 gabbro, 94 to 95% melt crystallization or 1% fusion of this mantle would best match the pattern and concentrations. The Rivera plate sample (D5-2int) does not have similarities to any patterns, probably because the

modeled source is the average depleted mantle (enriched + depleted mantle), whereas the source of this sample is exclusively the depleted mantle (N-MORB).

This modeling is simplistic as it only considers one source (the mantle) and only one process at time. However, if an average depleted mantle was the source, most samples could be generated by high degrees of crystallization and less probably low degrees of partial melting. The quartz-monzodiorite would be generated by low degrees of mantle melting.

## Rb-Sr AND Sm-Nd ISOTOPE SYSTEMATICS

Sample preparation for Rb-Sr and Sm-Nd isotope analyses was performed at the LUGIS facilities, Instituto de Geofísica, UNAM, following the procedures described by Villanueva (2011) and Pompa-Mera *et al.* (2013). The isotope dilution technique was applied to all samples that were analyzed by thermal ionization mass spectrometry (TIMS), except for samples Aq-1, ATG-1, D5-2Ext and D5-2Int (Valdez-Moreno, 2006), for which the concentrations determined by ICP-MS were used to calculate the  $^{87}\text{Rb}/^{86}\text{Sr}$  and  $^{147}\text{Sm}/^{144}\text{Nd}$  ratios (Table 2). The initial  $^{87}\text{Sr}/^{86}\text{Sr}$  and  $^{143}\text{Nd}/^{144}\text{Nd}$  ratios and  $\epsilon\text{Nd}$  values were calculated according to the ages obtained in this study and from the literature (Table 2). For the Jilotlán gabbros (JLT-8A, JLT-12, JLT-30-2, JLT-32, JLT-45, MS-25), an age of 114 Ma was used (see next section). For the basaltic dike (JLT-13C), the ~70 Ma eight sample Rb-Sr whole rock isochron age of the granitic rocks of the Jilotlán complex was applied (Schaaf, 1990). For the Tepalcaltepec gabbro (JLT-41), a ~100 Ma U-Pb zircon age of a granitoid from Tepalcaltepec was used (Salazar-Juárez, 2015). For the Manzanillo gabbros (MZ-3, MZ-4), a 70 Ma U-Pb zircon age was employed (Panseri, 2007). For the Aquila sample (Aq-1), a 57 Ma Rb-Sr biotite cooling age was available (Schaaf, 1990). As the age of meta-sandstone (ATG-1) is unknown, the oldest available K-Ar hornblende age of 118 Ma for the host rock (Tecalitlán Formation) was used (Bermúdez-Santana, 1994).

The Depleted Mantle (DM) Nd values used for model age ( $T_{\text{DM}}$ ) calculations are 0.513089 and 0.2128 for  $^{143}\text{Nd}/^{144}\text{Nd}$  and  $^{147}\text{Sm}/^{144}\text{Nd}$ , respectively, which correspond to mean values obtained from San Luis Potosí upper mantle xenoliths (Schaaf *et al.*, 1994). The present day Chondritic Uniform Reservoir (CHUR)  $^{143}\text{Nd}/^{144}\text{Nd}$  and  $^{147}\text{Sm}/^{144}\text{Nd}$  values used for ( $\epsilon\text{Nd}$ )<sub>i</sub> calculations are 0.512638 and 0.1967, respectively (Faure and Mensing, 2005).

Initial  $^{143}\text{Nd}/^{144}\text{Nd}$  vs.  $^{87}\text{Sr}/^{86}\text{Sr}$  ratios for all samples are plotted in Figure 10 and accompanied with data fields from Cordilleran Mexico (Puerto Vallarta batholith) and from the Andean and Japan volcanic arcs (Winter, 2001). The initial  $^{143}\text{Nd}/^{144}\text{Nd}$  values for the gabbros are less radiogenic than typical depleted mantle values (*e.g.*, Iherzolitic xenoliths in basanites from San Luis Potosí; Schaaf *et al.*, 1994) but still plot within the mantle array (Figure 10). Therefore, they could be obtained a) from a mantle wedge enriched in sediment/slab components by continuous subduction ( $<\text{Sm}/\text{Nd}$  than MORB), and/or b) the participation of crustal components ( $<\text{Sm}/\text{Nd}$  than mantle) mixed with mantle material. In this scenario, the Nd model ages ( $T_{\text{DM}}$ ) of all gabbros (averaging  $T_{\text{DM}} = \sim 500$  Ma) would indicate an average crustal residence age of all components involved in gabbro genesis.

The initial  $^{87}\text{Sr}/^{86}\text{Sr}$  values indicate very little participation of old continental crust ( $>\text{Rb}/\text{Sr}$ ) that would have enriched the mantle wedge by slab components, subducted sediments, or crustal contamination. Thus, magma generation processes included moderately evolved crust/slab components and/or sediments mixed with mantle material. As expected, the quartz-monzodiorite originated from a more evolved source than the gabbros. The Tepalcaltepec gabbro shows similar

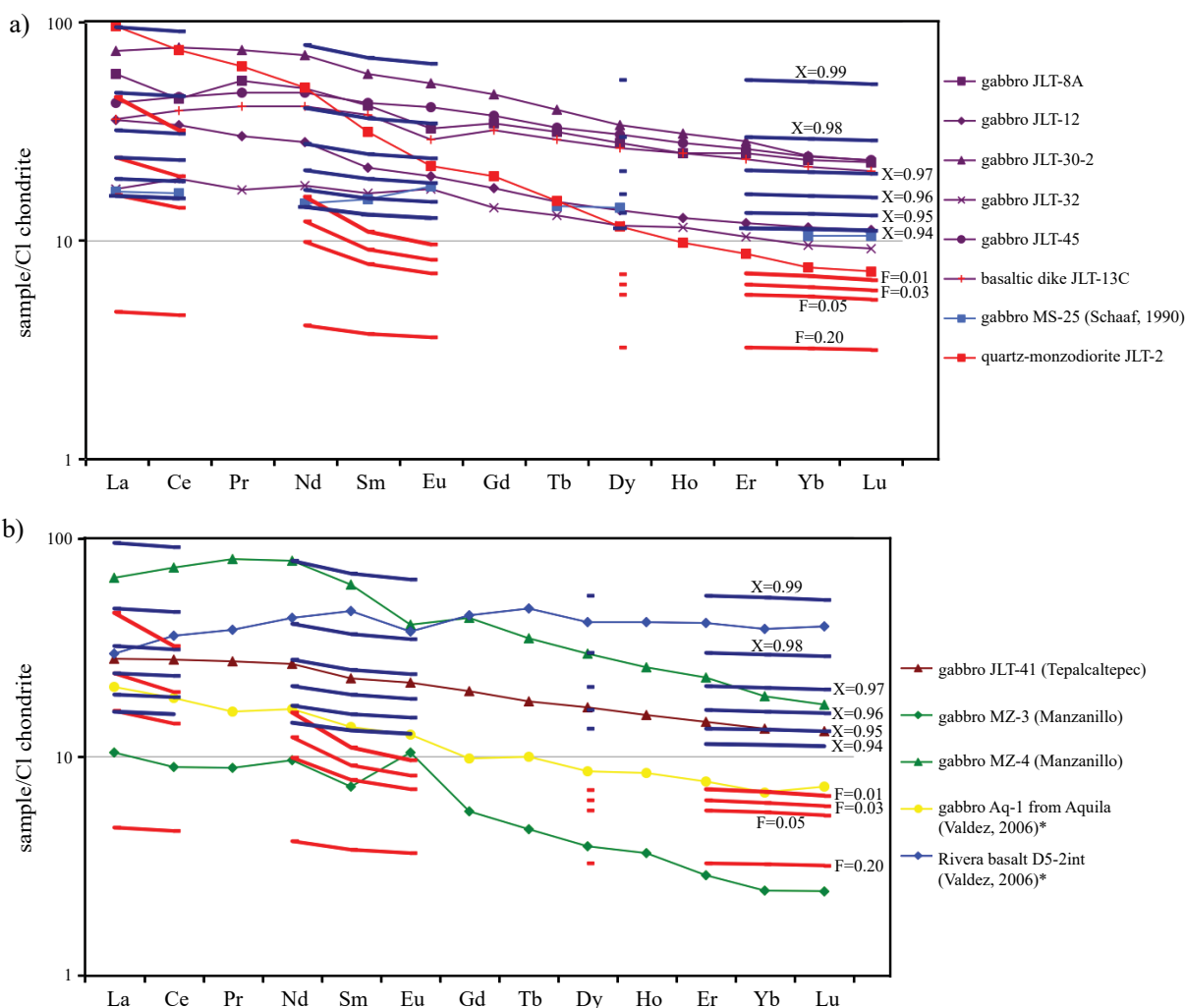


Figure 9. a) REE diagram of the gabbros and quartz-monzodiorite JLT-23 of the Jilotlán pluton and plots of the same elements for different degrees of batch melting ( $F$ ) and crystal fractionation ( $X$ ) for the melt of a plagioclase peridotite with the composition of the average depleted upper mantle according to Workman and Hart (2005). b) The same diagram for the Tepalcaltepec, Manzanillo, Aquila gabbros and the Rivera plate basalts. \*Valdez-Moreno (2006).

initial  $^{143}\text{Nd}/^{144}\text{Nd}$  values to those of Jilotlán, but with higher initial  $^{87}\text{Sr}/^{86}\text{Sr}$ , indicative for some secondary carbonate enrichment by alteration. Both Manzanillo (MZ) gabbros show initial Sr-Nd isotopic compositions very similar to Jilotlán. Therefore, their previously observed differences in trace element are probably due to different crystallization degrees, and less probably the result of different partial melting degrees (Figure 9b).

## GEOCHRONOLOGY

In order to determine the age of the gabbros and compare them to the surrounding granitoids ( $\sim 70$  Ma), a Jilotlán gabbro sample (JLT-12) was chosen to perform  $^{40}\text{Ar}/^{39}\text{Ar}$  geochronology on two types of hornblende (black and green). From this sample, and additionally from gabbro JLT-32, zircons were selected for U-Pb geochronology. The techniques and equipment of LUGIS at UNAM were used for mineral separation. Hornblende was isolated by handpicking and standard separation procedures (Villanueva, 2011) to guarantee inclusion-free crystals. Energy-dispersive X-ray spectroscopic analysis were performed on some crystals to test the purity of the concentrate at the Instituto de

Geología, UNAM. Approximately 80% of the crystals were hornblende and 20% clinopyroxene, which are K-free or have negligible K concentrations and have thus no influence on the  $^{40}\text{Ar}/^{39}\text{Ar}$  age.  $^{40}\text{Ar}/^{39}\text{Ar}$  analyses of these minerals were performed at the University of Alaska at Fairbanks, where the samples were further purified. Analytical procedures are described in York *et al.* (1981), Layer *et al.* (1987), and Layer (2000). Black and green JLT-12 hornblende separates show similar plateau ages of  $114.6 \pm 1.1$  Ma and  $111.0 \pm 1.1$  Ma, respectively (Figure 11; Tables A4, A5 of the Supplementary Material). The plateaus include more than 80% of  $^{39}\text{Ar}$  released during analysis. The positively sloped Ca/K and Cl/K diagrams evidence some alteration and argon loss in both samples, although this condition is more pronounced in the green hornblende with higher Ca/K ratios (Figure 11). Given the well-defined plateau, the  $114.6 \pm 1.1$  Ma and the  $111.0 \pm 1.1$  Ma hornblende ages are considered as cooling ages ( $540 \pm 40$  °C; Harrison and McDougall, 1980). However, the obtained ages could be minimum ages, considering a possible reset of the Ar-Ar system as a consequence of the granitoid intrusion. To prove this, zircon U-Pb geochronology was performed on the same and an additional sample (JLT-32).

As zircons are generally not very abundant in gabbros and mafic rocks, only a few crystals were obtained from both samples (19 crys-

tals for JLT-12 and 20 for JLT-32) using handpicking and standard procedures (without Wilfley table, Villanueva, 2011; Hernández *et al.*, 2012). The zircons were analyzed by LA-MC-ICP-MS at the University of Arizona (Table A6 of the Supplementary Material; Figure 12). Analytical procedures are described in Gehrels *et al.* (2006; 2008) and in Pompa-Mera *et al.* (2013). The individual ages, ranging from 104 to 123 Ma (Table A6 of the Supplementary Material) are mostly concordant. Zircons are considered as magmatic since no zoning was observed in cathodoluminescence pictures. TuffZirc ages (Ludwig and Mundil, 2002) were calculated using the Isoplot 3.6 Software (Ludwig, 2008). An age of 112.84 ± 1.20 - 1.72 Ma was obtained for gabbro JLT-12 and of 114.61 ± 1.34 - 0.93 Ma for gabbro JLT-32 (Figure 12).

The  $^{40}\text{Ar}/^{39}\text{Ar}$  hornblende ages and the U-Pb zircon age of JLT-12 are identical within standard deviations, indicating rapid cooling of the gabbroic magma. Considering the errors in the JLT-12 U-Pb age, as well the U-Pb zircon age of 114.6 ± 1.34/-0.93 Ma of sample JLT-32, the crystallization of the gabbros took place between 111.12 and 115.94 Ma. These ages also indicate a time span of at least 40 Ma between the gabbro formation and the emplacement of the surrounding granitoids, which were dated at 68 ± 12 Ma (eight point Rb-Sr whole rock isochron; Schaaf, 1990) and 54 ± 10 Ma (conventional U-Pb zircon age; Salazar-Juárez, 2015).

## DISCUSSION

### Petrogenesis

The mineralogy of all gabbroic samples resulted from a hydrated source (plagioclase with  $\text{An}_{50-68} + \text{Hbl} + \text{Cpx} \pm \text{Opx}$ ) with hornblende being by far the most abundant mafic mineral. The presence of clino-

pyroxene crystals surrounded by hornblende (Figures A2a, A3d) suggests hydration of the magmatic system after pyroxene crystallization. However, as some hornblende crystals are in contact with well-developed clinopyroxene crystals, hornblende growth directly from the magma is also a possible mechanism. Perhaps both, magmatic hornblende and secondary hydration occurred: biotitization of hornblende (Figure A2d) suggests a second hydration event, probably related to the granitoid intrusion.

All the gabbros were produced in a magmatic arc over a subduction zone, which is indicated by geochemical data (high Pb and Sr concentrations and higher LILE concentrations in comparison to HFSE or REE) and mineralogy (hornblende-rich gabbros with abundant water). On the other hand, the similar distributions and small differences in trace element concentrations of the gabbroic samples from Jilotlán, Tepalcaltepec, Aquila, and Manzanillo and their very similar isotopic ratios, evidence different magma generation processes from the same source, probably by different degrees of crystal fractionation. In comparison to the gabbros, the quartz-monzodiorite is magmatically slightly more evolved.

Geochemical and isotopic compositions of the gabbros and the quartz-monzodiorite underline the primitive magmatic character of this part of the Zihuatanejo Terrane. Nd model ages ( $T_{DM}$ ) around 500 Ma exclude the participation of old and evolved crustal components as it was observed further to the NW in the Puerto Vallarta batholith (0.6-1.6 Ga Nd ( $T_{DM}$ ) model ages; Schaaf, 1990). Subduction erosion processes (e.g., von Huene and Scholl, 1991) could have derived fragments of the volcanosedimentary cover of the Zihuatanejo Terrane (Jurassic-Cretaceous arc and sedimentary rocks) into the Wadati Benioff Zone and the mantle wedge accompanied by sediments of the oceanic lithosphere. Another possible crustal component could

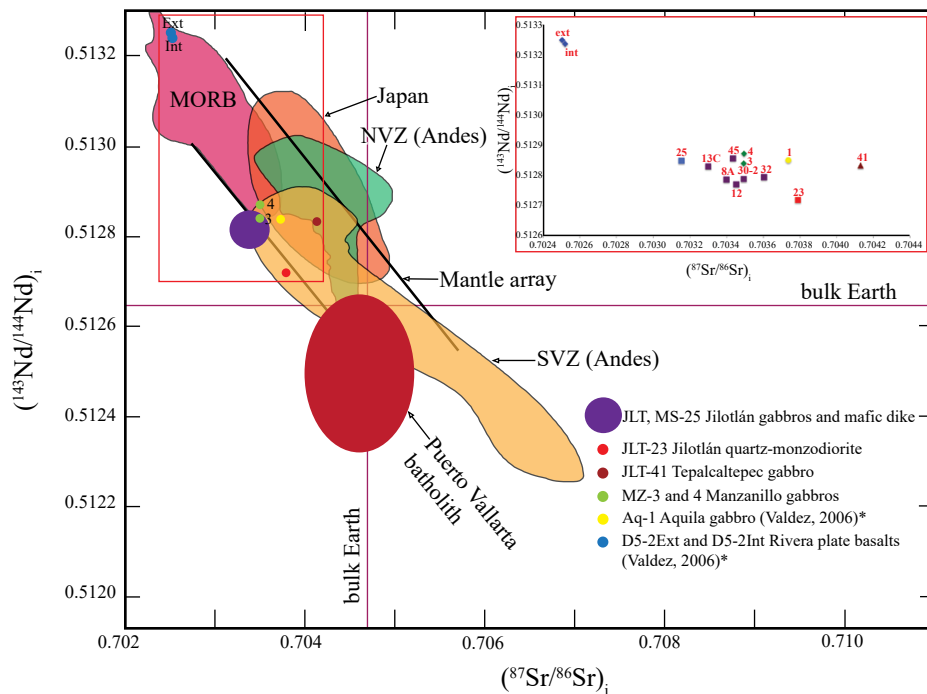


Figure 10.  $^{143}\text{Nd}/^{144}\text{Nd}$  vs.  $^{87}\text{Sr}/^{86}\text{Sr}$  diagram modified from Winter (2001) with initial (i) isotope ratios of the Jilotlán samples and those from previous studies. The inset shows in detail the samples within the Mantle Array field (red square). The MORB field is the average of different mid-ocean ridge basalts. The Japan field is an average of the Japanese island arc. NVZ and SVZ are the northern and southern volcanic zone of the Andes, respectively (all data from Winter (2001). The average Puerto Vallarta batholith values of Cordilleran Mexico are also displayed (Schaaf, 1990). All mentioned fields were graphed with their actual isotope ratios. \*Valdez-Moreno (2006).

Table 2. Isotopic ratios of <sup>87</sup>Rb/<sup>86</sup>Sr, <sup>87</sup>Sr/<sup>86</sup>Sr, <sup>147</sup>Sm/<sup>144</sup>Nd, <sup>143</sup>Nd/<sup>144</sup>Nd, εNd and their corresponding initial ratios marked with the i suffix. Nd model ages (T<sub>DM</sub>) are also shown.

Sample	Type of rock	<sup>87</sup> Rb/ <sup>86</sup> Sr	<sup>87</sup> Sr/ <sup>86</sup> Sr	1sd	2SE(M)	<sup>147</sup> Sm/ <sup>144</sup> Nd	<sup>143</sup> Nd/ <sup>144</sup> Nd	1sd	2SE(M)	εNd	1sd	( <sup>143</sup> Nd/ <sup>144</sup> Nd) <sub>i</sub>	(εNd) <sub>i</sub>	T <sub>DM</sub> (Ga)	Sample age (Ma)	Rb (ppm)	Sr (ppm)	Sm (ppm)	Nd (ppm)	
JLT-8A	microgabbro	0.182	0.703694	38	11	0.703399	0.156	0.512903	16	4	5.17	0.31	0.512787	5.77	0.497	114	21.10	334.99	6.37	24.74
JLT-12	microgabbro	0.103	0.703620	36	9	0.703453	0.147	0.512881	16	4	4.74	0.31	0.512772	5.47	0.480	114	17.63	495.25	3.00	12.38
JLT-13C	basaltic dike	0.048	0.703347	35	9	0.703299	0.171	0.512909	20	6	5.29	0.39	0.512830	5.51	0.665	70	5.85	353.15	5.62	19.81
JLT-23	quartz-monzodiorite	0.362	0.704149	38	10	0.703789	0.119	0.512774	20	5	2.65	0.39	0.512720	3.35	0.511	70	86.97	694.34	4.87	24.80
JLT-30-2	microgabbro	0.163	0.703758	40	11	0.703493	0.153	0.512903	15	4	5.17	0.29	0.512789	5.81	0.475	114	23.40	414.52	8.28	32.72
JLT-32	microgabbro	0.144	0.703837	38	10	0.703603	0.173	0.512924	19	5	5.58	0.37	0.512795	5.93	0.631	114	22.13	443.95	3.19	11.16
JLT-41	microgabbro	0.404	0.704704	36	10	0.704130	0.163	0.512941	20	5	5.91	0.39	0.512834	6.34	0.456	100	45.77	327.91	3.50	12.95
JLT-45	microgabbro	0.038	0.703497	35	10	0.703435	0.169	0.512984	17	5	6.75	0.33	0.512858	7.15	0.366	114	5.06	380.48	6.22	22.24
MZ-3	microgabbro	0.005	0.703498	30	8	0.703493	0.154	0.512911	23	8	5.33	0.45	0.512840	5.70	0.465	70	2.34	1446.50	1.14	4.47
MZ-4	gabbro	0.042	0.703536	37	10	0.703495	0.144	0.512939	16	4	5.87	0.31	0.512873	6.34	0.335	70	13.13	910.58	9.64	40.37
MS-25	gabbro	0.223	0.703515	35	9	0.703154	0.185	0.512988	29	7	6.83	0.58	0.512850	7.00	0.558	114	25.00	318.00	2.50	8.20
Aq-1	gabbro	0.054	0.703780	35	9	0.703736	0.162	0.512912	17	5	5.34	0.34	0.512852	5.60	0.532	57	11.77	628.40	2.02	7.54
ATG-1	meta-sandstone	43.30	0.751693	34	9	0.679078	0.187	0.512721	22	6	1.62	0.43	0.512576	1.76	2.202	118	232.92	15.63	1.81	5.84
D5-2Ext	Rivera basalt	0.093	0.702506	39	10	0.702504	0.208	0.513251	18	5	11.96	0.35	0.513249	11.96	-	1.4	5.66	175.50	8.05	23.40
D5-2Int	Rivera basalt	0.314	0.702526	41	11	0.702520	0.209	0.513239	19	5	11.72	0.37	0.513237	11.72	-	1.4	16.01	147.65	6.82	19.77

Sr, Nd and Sm isotope ratios were determined using a Finnigan MAT262 thermal ionization mass spectrometer (TIMS) equipped with eight Faraday collectors, installed at LUGIS, Instituto de Geofísica, UNAM. Isotopic measurements were made in static collection mode. Analyses of Rb were carried out in dynamic mode using a single collector NBS mass spectrometer at the Instituto de Geología, UNAM. Rb, Sr, Sm, and Nd were loaded as chlorides and measured as metallic ions. Standard deviations (1sd = ±1σ<sub>abs</sub>) refer to the last two digits. Standard error of the mean (2SE(M) = 2σ<sub>abs</sub>√n) values were calculated from 60 individual isotopic determinations for Sr and Nd, 40 for Rb, and 20 for Sm. The measured <sup>87</sup>Sr/<sup>86</sup>Sr values were normalized to a <sup>86</sup>Sr/<sup>88</sup>Sr value of 0.1194, and those of <sup>143</sup>Nd/<sup>144</sup>Nd to a <sup>146</sup>Nd/<sup>144</sup>Nd ratio of 0.7219. <sup>87</sup>Sr/<sup>86</sup>Sr of the NBS987 and <sup>143</sup>Nd/<sup>144</sup>Nd of the La Jolla standards measured throughout this study were 0.710237 ± 23 (1σ<sub>abs</sub>, n = 391) and 0.511867 ± 25 (1σ<sub>abs</sub>, n = 204), respectively. Rb concentrations were obtained by isotope dilution using a <sup>87</sup>Rb spike. Sr, Nd and Sm concentrations were obtained by isotope dilution using a combined <sup>84</sup>Sr-<sup>145</sup>Nd-<sup>149</sup>Sm spike. Relative uncertainty for <sup>87</sup>Rb/<sup>86</sup>Sr was ±2% and for <sup>147</sup>Sm/<sup>144</sup>Nd ±1.5% (1σ). Relative reproducibility (1σ) for Rb, Sr, Sm and Nd concentrations was ±4.5%, ±1.8%, ±3.2%, and ±2.7%, respectively. Total procedure blanks were 0.22 ng for Rb, 4.8 ng for Sr, 0.20 ng for Sm, and 0.71 ng for Nd.

be the mafic lower crust. The existence of hornblende rich gabbros and the presence of plagiogranites with similar ages to the gabbros in the northern part of the Jilotlán pluton (Salazar-Juárez, 2015) support the existence of at least 20 km thick primitive crust to allow magma differentiation. On the other hand, magmatic activity involving pure mantle material indeed occurred in the ultramafic body (duniticlinopyroxenite) of El Tamarindo in the Petatlán-Papanao area, with an <sup>40</sup>Ar/<sup>39</sup>Ar hornblende age of ~112 Ma (Delgado-Argote et al., 1992), which is identical to the age of the Jilotlán gabbros. Given the geochemical features, isotopic ratios and T<sub>DM</sub> ages of all samples, the source of the gabbros is constrained to be most likely a result of partial melting of mantle material enriched by sediments/fluids from the slab with some participation of primitive crustal components. The more evolved quartz-monzodiorite JLT-23 could have been generated by partial melting of mafic crust alone or from a combination of mantle with subduction related and mafic crustal components, with later fractional crystallization in both cases. However, a greater amount of subduction or crustal components was involved in the genesis of the quartz-monzodiorite compared to the gabbros.

The modeled REE behavior using the hypothetical depleted mantle as the only source shows that high degrees of crystal fractionation partially reproduce the patterns and the different element concentrations of the gabbros. The quartz-monzodiorite is partially reproduced only by low degrees of partial melting from the same depleted source.

### Geochronology

The ~40 Ma time span separating the gabbro and granitoid intrusions indicates that the gabbros in the study area were not comagmatic with the granitoids, although both were produced by subduction processes. The gabbros experienced very rapid cooling as the Ar-Ar hornblende and the U-Pb zircon ages are identical within errors, considering their 540±40 °C and ~750 °C closure temperatures, respectively. This implies that these rocks crystallized in a shallow crustal zone and/or were uplifted very rapidly. The plagioclase inclusions observed in some clinopyroxene and hornblende crystals could be the result of exsolution processes during rapid uplift. The granitoids intruded the gabbros ~40 Ma later and did not reheat them above ~540 °C, a fact that is also supported by field relations. These granites could be part of a batholith, also emplaced in shallow crustal levels. The <sup>40</sup>Ar/<sup>39</sup>Ar hornblende and U-Pb zircon crystallization ages suggest that the Jilotlán gabbros can be considered as the igneous roots of the hosting Tecalitlán Formation from which a 118 Ma K-Ar hornblende age was reported (Bermúdez-Santana, 1994).

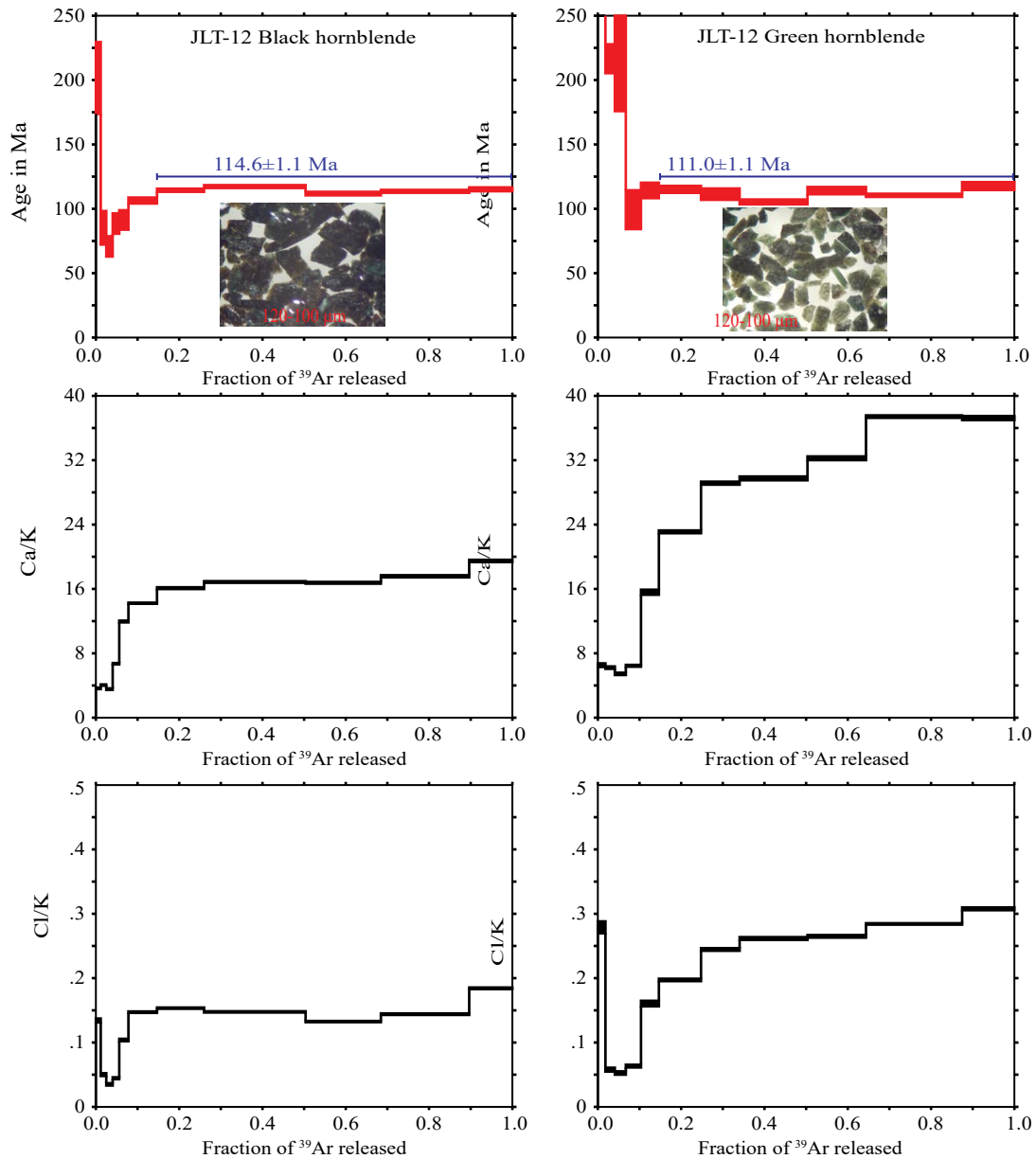


Figure 11. Step heating spectrum for JLT-12 black and green hornblende: age versus  $^{39}\text{Ar}$  released fraction (in red) and steps to define the plateau ages (in blue); also shown are Ca/K and Cl/K ratios versus  $^{39}\text{Ar}$  released for both minerals.

**Regional tectonics**

When comparing the Sr-Nd isotopic signatures of all Jilotlán samples to those from other magmatic arcs (Figure 10), similarities to the Southern Volcanic Zone (SVZ) of the Andes are observable. The SVZ shows calc-alkaline and mid-K geochemical characteristics with relatively flat HREE patterns (Winter, 2001 and references therein). The SVZ crust is 30 to 35 km thick in average, mainly of Mesozoic and Cenozoic ages with geochemical affinities to island arcs and oceanic crust, but in an undoubtedly continental arc setting that is probably similar to the Jilotlán area ~114 Ma ago.

The Jilotlán gabbros were generated during the Early to middle Cretaceous (Barremian-Albian) arc event, considered as extensional (Centeno-García, 2005; Centeno-García *et al.*, 2008, 2011; Martini *et al.*, 2011). The extension could have allowed mantle magmas to ascend through the thinned and geochemically primitive basement crust to

produce the gabbros. As discussed above, a pure mantle source is less likely. The gabbros could have been generated by partial melting of the mantle and emplaced along faults, whereas the plagiogranites of the same age (north of Jilotlán) would be derived from partial melting of thicker crustal blocks and/or from fractional crystallization of underplating mafic magmas ascending through the faulted blocks. Ultramafic rocks like those of Petatlán-Papanao were generated from pristine mantle material emplaced through deeper/wider faults without crustal contamination. How and where the basal primitive crust was created is unknown, but it was a part of or closely located to continental Mexico prior to the deposition of the Arteaga complex in the Late Permian (before ~260 Ma). The accretion of Arteaga to continental Mexico occurred in the uppermost Early to Middle Jurassic (183 Ma–163 Ma; Elías-Herrera *et al.*, 2000; Centeno-García *et al.*, 2011).

Early Cretaceous magmatism in an extensional regime is also

documented during the opening and evolution of the Arperos basin (Martini *et al.*, 2011; 2014) in central (Guanajuato) and southern (Santo Tomás-Arcelia, Figure 1b) Mexico. Peraluminous rhyodacitic dikes and lava flows were emplaced along the Guerrero Terrane and continental mainland margins during the Tithonian to Barremian (150-125 Ma) (Martini *et al.*, 2011; 2014). During this time period, the Arperos basin was still floored by continental rocks or sediments, as is suggested by inherited Paleozoic and Precambrian zircons. Instead, intraplate-like and MORB basaltic flows dominated in the Aptian-Cenomanian (125-94 Ma), which suggests spreading within the Arperos basin. Its closure occurred in the late Cenomanian as the Guerrero Terrane was accreted back to continental Mexico (Martini *et al.*, 2014). During the

Tithonian-Aptian (150-112 Ma), between Guanajuato and Arcelia, the primitive calc-alkaline El Paxtle-Palmar Chico-Teloloapan magmatic arc was active in the Guerrero Terrane (Martini *et al.*, 2011; 2014). It had a basaltic to andesitic composition, with scarce felsic volcanic activity. In this scenario, the Jilotlán gabbros would be contemporaneous with the intraplate and MORB basalts (Aptian-Cenomanian). This suggests that the locus of magmatism within the Guerrero Terrane primitive arc migrated from central and southern Mexico towards the Jilotlán area during the Aptian (125-114 Ma) during regional extensional tectonics.

The quartz-monzodiorite was formed during the Santonian-Maastrichtian arc event (Centeno-García *et al.*, 2011) that is considered of compressional character. The compression could have thickened the

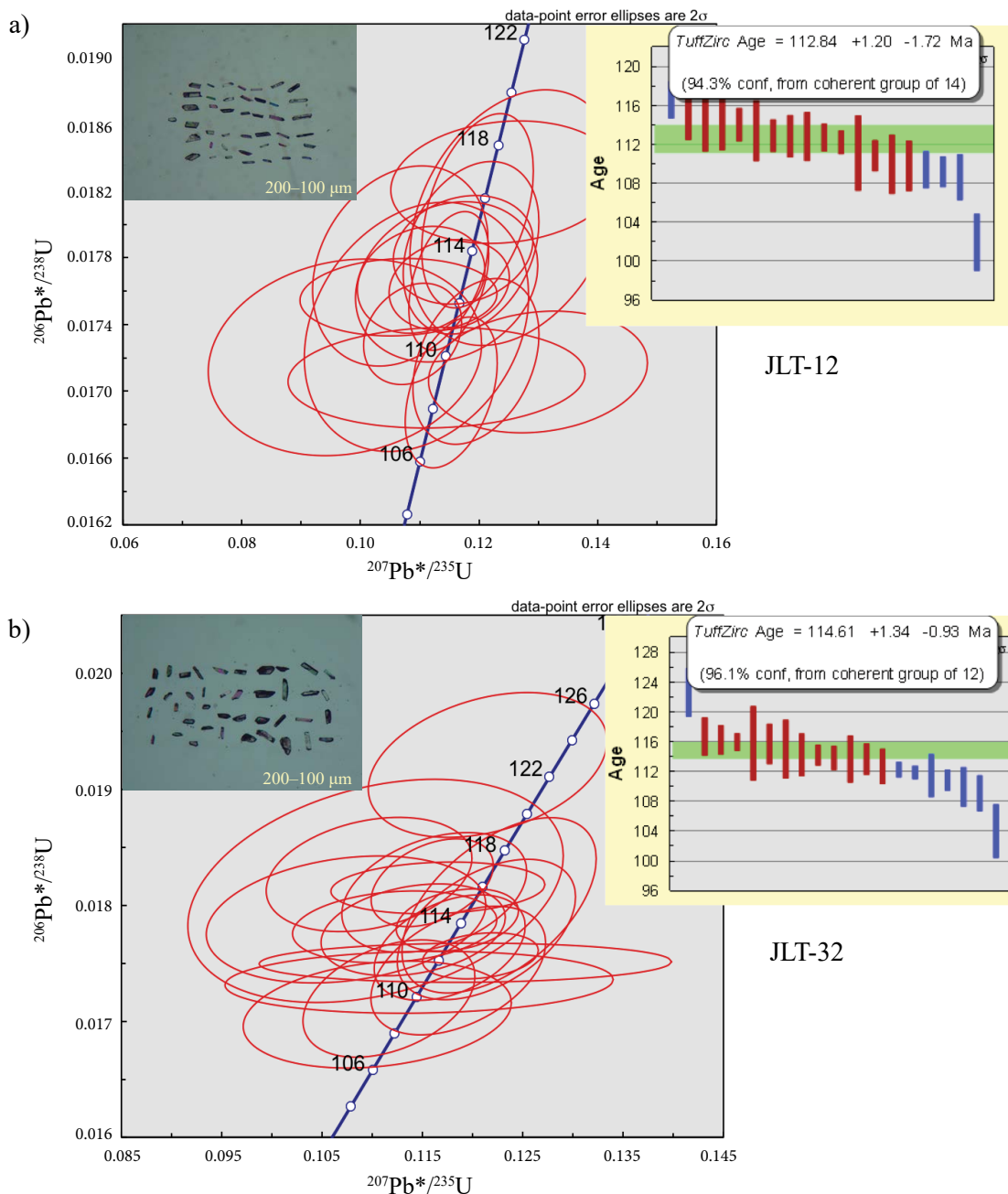


Figure 12.  $^{206}\text{Pb}^*/^{238}\text{U}$  vs.  $^{207}\text{Pb}^*/^{235}\text{U}$  Concordia diagrams for zircons from JLT-12 (a) and JLT-32 (b) gabbros. Error ellipsoids correspond to  $2\sigma$  errors. To the right, the age distributions are also shown in TuffZirc diagrams with  $2\sigma$  errors. Some binocular microscope photographs of the analyzed crystals are also displayed.

crust and allowed higher crustal partial melting degrees and magma differentiation, with less direct participation of mantle material. The formation of the quartz-monzodiorite from such thickened crust explains well its different evolution compared to the gabbros.

The very primitive character of the crustal gabbros studied in this work, confirms the existence of a basement that is magmatically poorly evolved without old crustal components ( $\epsilon\text{Nd}$ , up to  $\sim+7$  and  $T_{\text{DM}}$  up to  $\sim 0.7$  Ga ( $\sim 0.50$  Ga average)). This differs substantially from the basement underneath the Puerto Vallarta batholith ( $\sim 100$  Ma) with  $\epsilon\text{Nd}$ , parameters down to  $\sim -7$  and  $T_{\text{DM}}$  up to  $\sim 1.55$  Ga (Figure 10, Table 2), suggesting a tectonic limit. An alternative interpretation would be the presence of a lithospheric scale fault that facilitated the emplacement of mafic magmas without significant contamination by continental crust (e.g., Kirsch *et al.*, 2012). In this case, the fault would not have apparently affected the Puerto Vallarta batholith. However, no local or regional structural investigations were performed in this study to prove this.

Regionally, gabbros are abundant within the mid-Cretaceous Peninsular Ranges batholith (PRB) in southern and Baja California (Kimbrough *et al.*, 2015), ranging in composition from cumulate olivine gabbro, gabbro-norite to hornblende gabbro. A western zone within this batholith contains abundant gabbros whereas in the eastern zone gabbro is rare ( $<1\%$  of the outcrop area). The U-Pb zircon crystallization ages range from  $130.5 \pm 1.5$  Ma to  $100.2 \pm 3.0$  Ma for the western zone gabbros, which is consistent with the  $\sim 30$  Ma time for the emplacement of the overall western zone batholith. In contrast, the eastern zone gabbros have crystallization ages from  $109.4 \pm 2.9$  Ma to  $97.8 \pm 2.3$  Ma that predate the ca. 92–98 Ma tonalite-trondhjemite-granodiorite batholith flareup of the eastern zone, and may have played a role in crustal thickening and flareup triggering. The whole rock and trace element compositions of all the gabbros closely match signatures for high-alumina olivine tholeiite, arc basalt, and basaltic andesite from modern arcs. Nearly flat REE patterns for western and eastern zone gabbros reflect derivation from a common partially contaminated depleted mantle source. This contrasts with the geochemical and isotopic data of the granitoids, which reflect progressively deeper partial melting of mafic source rocks from west to east with additional input from a radiogenic end member in the eastern side of the batholith.

In this scenario, the Jilotlán gabbros ages ( $\sim 114$  Ma) are coeval with both the western and eastern gabbro belts of the PRB ( $\sim 130$ – $100$  Ma). The presence of some plagiogranites north of Jilotlán of the same age as the Jilotlán gabbros is also observed in the western zone gabbros in the PRB, where the crust is probably thinner than in the eastern zone (Kimbrough *et al.*, 2015). These similarities together with paleo-reconstructions, where Baja California was part of continental Mexico, suggest a regional magmatic arc setting with prevalent gabbroic magma generation in the PRB, and, in contrast, apparently lower abundances between Puerto Vallarta and Acapulco, as documented by the Jilotlán gabbros and the Petatlán-Papanoa ultramafic rocks. This scenario fits well with the contemporaneous extensional arc documented in the Zihuatanejo terrane (Centeno-García *et al.*, 2011) where mafic magmas were emplaced in a magmatic arc setting due to thinned crust and deep faults. The central Jilotlán plagiogranites ( $\sim 70$  Ma) are younger than the PRB gabbros and tonalitic-trondhjemitic granitoids ( $>92$  Ma) and form part of the compressional arc documented in the Zihuatanejo Terrane. In this context, the scenario is similar to the eastern PRB, where the gabbros could have thickened the crust in addition to regional compression, constituting the source from which plagiogranites were generated.

This study supports the hypothesis that a long-lived subduction zone (at least since the Early Cretaceous) is responsible for the formation of continental arc rocks from very primitive sources. The primitive

rocks in the Jilotlán area are the result of mantle magmas formed above a subduction zone and mixed with geochemically primitive oceanic type basement rocks. They were emplaced in a thinned continental crust due to extensional tectonics. This has been geochemically documented for the Zihuatanejo Terrane, part of the Guerrero Terrane.

## CONCLUSIONS

1. The Jilotlán gabbros are part of the Guerrero Terrane, with primitive geochemical characters in the study area, and differ substantially from the to the NW neighboring Puerto Vallarta intrusives. Based on the available studies, the Jilotlán gabbros are part of the Barremian-Albian Zihuatanejo extensional arc, whereas the granitoids of Jilotlán would be part of the Santonian-Maastrichtian compressional arc, both generated by variations in the slab geometries of a single subduction zone in a continental arc setting. These tectonic scenarios could explain the geochemical features distinguishing the gabbros from the granitoids by heterogeneities in crustal thickness.

2. Trace element distributions and Sr-Nd isotopic ratios of the gabbros show that they are part of a magmatic arc generated from a homogeneous source, most probably essentially by partial melting of mantle material enriched by sediments/fluids derived from the slab with some participation of primitive crustal components. The geochemical variations could be explained by different degrees of fractional crystallization and less probably by different degrees of partial melting of this primitive source.

3. A magmatic hiatus of  $\sim 40$  Ma separates the Jilotlán gabbros (114 Ma) from the intruding granodiorites and tonalites (68 Ma), which confirms that these units are not cogenetic.

4. The gabbros could be the roots of the host rock Tecalitlán Formation, emphasized by within error identical ages ( $\sim 114$  Ma and  $\sim 118$  Ma, respectively).

5. The gabbros crystallized and cooled down very rapidly as there is no substantial differences between the Ar-Ar hornblende and U-Pb zircon ages within the same sample. This evidences a shallow emplacement and/or rapid uplift. As the gabbros were intruded by the granitoids, this implies that latter were also emplaced shallowly or exhumed rapidly.

6. Similarities in age and inferred petro-tectonic settings of the Jilotlán gabbros with the gabbros of the Peninsular Ranges batholith and the ultramafic rocks from the Petatlán-Papanoa region could indicate that gabbros and mafic rocks constitute a common feature in extensional continental arc settings related to crustal thinning.

## ACKNOWLEDGEMENTS

Field work and all analyses for this paper were supported by DGAPA-PAPIIT Project IN115106 “Evolución tectonomagmática de los plagiogranitos de Manzanillo, Colima y Jilotlán, Jalisco” to P.S. This publication is also partially supported by the DGAPA-PASPA sabbatical grant to P.S. We thank Rufino Lozano and Patricia Girón for XRF analyses (LUGIS), Ofelia Pérez (CGEO) for ICP-MS data, Juan Julio Morales and Vianney Meza for isotopic measurements (LUGIS). Thanks to Bodo Weber and Valerie Pompa for U-Pb age determinations performed at the Arizona LaserChron Center, with access provided by George Gehrels and Joaquín Ruíz, and to Mark Pecha, who was in charge of the LA-MC-ICP-MS instrument at the LaserChron Center during our measurements. Thanks to Paul Layer and Jeff Benowitz for Ar-Ar age determinations in the Geochronology Laboratory of the University of Alaska at Fairbanks. Thanks to Margarita Reyes for SEM

analysis (IGL), to Consuelo Macías (IGL) for help with sample preparation and to Jesús Solé (IGL) for advice on hornblende concentrates. Thanks to Carles Canet (IGF) and Lilia Arana (IGF) for providing access to the SEM tabletop microscope. Reviews of Moritz Kirsch and Uwe Martens helped to improve substantially the original manuscript. Special thanks to Teresa Orozco for the exhaustive review of the last version of the manuscript.

## APPENDIX. SUPPLEMENTARY MATERIAL

Figures A1 to A5 (photographs showing petrographic details) and Tables A1 (major element concentrations), A2 (trace element concentrations), A3 (partition coefficients used in model calculations), A4 (results of Ar-Ar step-heating experiments), A5 (summary of  $^{40}\text{Ar}^*/^{39}\text{Ar}$  geochronology), A6 (U-Pb zircon data) can be found at the journal web site <<http://rmcg.unam.mx/>>, in the table of contents of this issue.

## REFERENCES

- Alenclaster, G., 1986, Nuevo rudista (Bivalvia-Hippuritacea) del Cretácico Inferior de Pihuamo, Jalisco: *Boletín de la Sociedad Geológica Mexicana*, 47 (1), 47-60.
- Altamira-Areyán, A., 2002, Las litofacies y sus implicaciones de la cuenca sedimentaria Cutzamala-Tiquicheo, Estado de Guerrero y Michoacán, México: México, Universidad Nacional Autónoma de México, Instituto de Geología, M.Sc. Thesis, 79 pp.
- Barbarin, B., 2005, Mafic magmatic enclaves and mafic rocks associated with some granitoids of the central Sierra Nevada batholith, California: nature, origin and relations with the hosts: *Lithos*, 80, 155-177.
- Benammi, M., Centeno-García, E., Martínez-Hernández, E., Morales-Gámez, M., Urrutia-Fucugauchi, J., Tolson, G., 2005, Presencia de dinosaurios en la Barranca Los Bonetes en el sur de México (Región de Tiquicheo, Estado de Michoacán) y sus implicaciones cronoestratigráficas: *Revista Mexicana de Ciencias Geológicas*, 22, 429-435.
- Bermúdez-Santana, J.C., 1994, Estratigrafía de una secuencia volcanosedimentaria del Cretácico Inferior de la región de Tepalcaltepec-Coalcomán, Michoacán, integrando métodos bioestratigráficos y radiométricos: México, D.F., Instituto Politécnico Nacional, Escuela Superior de Ingeniería y Arquitectura, M.Sc. Thesis, 103 pp. (unpublished).
- Bissig, T., Mortensen, J.K., Tosdal, R.M., Hall, B.V., 2008, The rhyolite-hosted volcanogenic massive sulfide district of Cuale, Guerrero Terrane, west-central Mexico: Silver-rich base metal mineralization emplaced in a shallow marine continental margin setting: *Economic Geology*, 103, 141-159.
- Buitrón, B.E., 1986, Gasterópodos del Cretácico (Aptiano Tardío-Albiano Temprano) del Cerro de Tuxpan, Jalisco: *Boletín de la Sociedad Geológica Mexicana*, 47 (1), 17-32.
- Campa, M.F., Coney, P. J., 1983, Tectono-stratigraphic terranes and mineral resource distributions in Mexico: *Canadian Journal of Earth Sciences*, 20, 1040-1051.
- Campa, M.F., Ramírez, J., Bloome, C., 1982, La secuencia volcánico-sedimentaria metamorizada del Triásico (Ladiniano-Cárnico) de la región de Tumbiscatio, Michoacán, in VI Convención Geológica Nacional: Sociedad Geológica Mexicana, Resúmenes, p. 48.
- Centeno-García, E., 1994, Tectonic evolution of the Guerrero Terrane, western Mexico: Tucson, University of Arizona, Ph.D. Thesis, 220 pp.
- Centeno-García, E., 2005, Review of Upper Paleozoic and Lower Mesozoic stratigraphy and depositional environments of central and west Mexico: Constraints on terrane analysis and paleogeography, in Anderson, T.H., Nourse, J.A., McKee, J.W., Steiner, M.B. (eds.), *The Mojave-Sonora Megashield Hypothesis: Development, Assessment, and Alternatives*, Geological Society of America, Special Paper 393, 233-258.
- Centeno-García, E., Silva-Romo, G., 1997, Petrogenesis and tectonic evolution of central México during Triassic-Jurassic time: *Revista Mexicana de Ciencias Geológicas*, 14, 244-260.
- Centeno-García, E., Ruíz, J., Coney, P., Patchett, J.P., Ortega, G.F., 1993, Guerrero Terrane of Mexico: Its role in the Southern Cordillera from new geochemical data: *Geology*, 21, 419-422.
- Centeno-García, E., Corona-Chávez, P., Talavera-Mendoza, O., Iriondo, A., 2003, Geology and tectonic evolution of the Western Guerrero Terrane—A transect from Puerto Vallarta to Zihuatanejo, México, in *Geologic Transects across Cordillera México*, Guidebook for Field Trips of the 99th GSA Cordilleran Section Meeting: Universidad Nacional Autónoma de México, Instituto de Geología, Publicación Especial (1), 201-228.
- Centeno-García, E., Guerrero-Suástegui M., Talavera-Mendoza O., 2008, The Guerrero Composite Terrane of western Mexico: Collision and subsequent rifting in a supra-subduction zone: *Geological Society of America, Special Paper* 436, 279-308.
- Centeno-García, E., Busby, C., Busby, M., Gehrels, G., 2011, Evolution of the Guerrero composite terrane along the Mexican margin, from extensional fringing arc to contractional continental arc: *Geological Society of America Bulletin*, 123, 1776-1797.
- Corona-Chávez, P., 1999, El basamento litológico y tectónico del Estado de Michoacán, in Garduño-Monroy V.H., Corona-Chávez P., Israde-Alcántara I., Mennella L., Arreygüe, E., Bigioggero B., Chiesa S. (eds.) *Carta Geológica de Michoacán escala 1:250,000*: Universidad Michoacana de San Nicolás de Hidalgo, 10-29.
- Cox, K.G., Bell, J.D., Pankhurst, R.J., 1979, *The Interpretation of Igneous Rocks*: London, George, Allen and Unwin, 464 pp.
- Cuevas, S.F., 1981, *Prospecto Tepalcaltepec*: México, D.F., Petróleos Mexicanos, IGPR-164, reporte interno (no publicado).
- De Cserna, Z., 1978, Notas sobre la geología de la región comprendida entre Iguala, Ciudad Altamirano y Temascaltepec, Estados de Guerrero y México: *Sociedad Geológica Mexicana, Libro Guía de la Excursión geológica a Tierra Caliente*, 1-25.
- De Cserna, Z., Palacios-Nieto, M., Pantoja-Alor, J., 1978, Relaciones de facies de las rocas cretácicas en el noroeste de Guerrero y en áreas colindantes de México y Michoacán: *Revista del Instituto de Geología*, 2 (1), 8-18.
- Delgado-Argote, L.A., López-Martínez, M., York, D., Hall, C. M., 1992, Geologic framework and geochronology of ultramafic complexes of southern México: *Canadian Journal of Earth Sciences*, 29, 1590-1604.
- Dickinson, W.R., Lawton, T.F., 2001, Carboniferous to Cretaceous assembly and fragmentation of Mexico: *Geological Society of America Bulletin*, 113, 1142-1160.
- Eliás-Herrera, M., Sánchez-Zavala, J.L., 1992, Tectonic implications of a mylonitic granite in the lower structural levels of the Tierra Caliente Complex (Guerrero Terrane), Southern Mexico: *Revista Mexicana de Ciencias Geológicas*, 9, 113-125.
- Eliás-Herrera, M., Ortega-Gutiérrez, F., 1997, Petrology of high-grade pelitic xenoliths in an Oligocene rhyodacitic plug: precambrian crust beneath the southern Guerrero Terrane?: *Revista Mexicana de Ciencias Geológicas*, 14, 101-109.
- Eliás-Herrera, M., Sánchez-Zavala, J.L., Macías-Romo, C., 2000, Geologic and geochronologic data from the Guerrero terrane in the Tejuipulco area, southern Mexico: new constraints on its tectonic interpretation: *Journal of South American Earth Sciences*, 13, 355-375.
- Faure, G., Mensing T., 2005, *Isotopes, Principles and Applications*: Nueva York, John Wiley & Sons, 897 pp.
- Ferrari, L., Bergomi, M., Martini, M., Tunesi, A., Orozco Esquivel, T., López Martínez, M., 2014, Late Cretaceous-Oligocene magmatic record in southern Mexico: the case for a temporal slab window along the evolving Caribbean-North America-Farallon triple boundary: *Tectonics*, 33, 1738-1765.
- Freydier, C., Lapiere, H., Briquieu, L., Tardy, M., Coulon, C., and Martínez, J., 1997, Volcaniclastic sequences with continental affinities within the Late Jurassic- Early Cretaceous intraoceanic arc terrane (western Mexico): *Journal of Geology*, 105, 483-502.
- Gastil, R.G., Krummenacher, D., Jensky II, W.A., 1978, *Reconnaissance geology of west-central Nayarit, Mexico*: Geological Society of America Map Chart Series, MC-24, 1-8.
- Gehrels, G., Valencia, V., Pullen, A., 2006, Detrital zircon geochronology by Laser-Ablation Multicollector ICPMS at the Arizona Laserchron Center, from Geochronology: in Olszewski, T. (ed.), *Emerging Opportunities, Paleontological Society Short Course*: Philadelphia, PA., The

- Paleontological Society, Paleontological Society Papers, 67-76.
- Gehrels, E., Victor, A.V., Ruiz, J., 2008, Enhanced precision, accuracy, efficiency, and spatial resolution of U-Pb ages by laser ablation-multicollector-inductively coupled plasma-mass spectrometry: *Geochemistry, Geophysics, Geosystems*, 9, Q03017.
- Gómez-Tuena, A., Langmuir, C.H., Goldstein, S.L., Straub, S.M., Ortega-Gutiérrez, F., 2007, Geochemical evidence for slab melting in the Trans-Mexican Volcanic Belt: *Journal of Petrology*, 48 (3), 537-562.
- Grajales-Nishimura, M., López-Infanzón, M., 1984, Estudio petrogenético de las rocas ígneas y metamórficas en el Prospecto Tomatlán-Guerrero-Jalisco: Instituto Mexicano del Petróleo, Subdirección de Tecnología y Exploración, Proyecto C-1160 (unpublished).
- Harrison, T. M., McDougall, I., 1980, Investigations of an intrusive contact, northwestern Nelson, New Zealand: II. Diffusion of radiogenic and excess  $^{40}\text{Ar}$  in hornblende revealed by  $^{40}\text{Ar}/^{39}\text{Ar}$  age spectrum analysis: *Geochimica et Cosmochimica Acta*, 44, 2005-2020.
- Hernández-Treviño, T., Schaaf, P., Solís-Pichardo, G., Villanueva-Lascurain, D., Meza-García, V., 2012, Practical zircon separation technique for U-Pb geochronology: VIII South American Symposium on Isotope Geology, Medellín, Colombia, Abstracts.
- Irvine, T.N., Baragar, W.R., 1971, A guide to the chemical classification of the common volcanic rocks: *Canadian Journal of Earth Sciences*, 8, 523-548.
- Kimbrough, D.L., Grove, M., Morton, D.M., 2015, Timing and significance of gabbro emplacement within two distinct plutonic domains of the Peninsular Ranges batholith, southern and Baja California: *Geological Society of America Bulletin*, 127 (1/2), 19-37.
- Kirsch, M., Keppie, D.J., Murphy, B.J., Solari, L.A., 2012, Permian-Carboniferous arc magmatism and basin evolution along the western margin of Pangea: Geochemical and geochronological evidence from the eastern Acatlán Complex, southern Mexico: *Geological Society of America Bulletin*, 124 (9-10), 1607-1628.
- Lapierre, H., Ortiz, L.E., Abouchami, W., Monod, O., Coulon, C., Zimmermann, J.L., 1992, A crustal section of an intra-oceanic island arc—the Late Jurassic-Early Cretaceous Guanajuato magmatic sequence, central Mexico: *Earth Planetary Science Letters*, 108, 61-77.
- Layer, P.W., 2000, Argon-40/Argon-39 age of the El'gygytyn impact event, Chukotka, Russia: *Meteoritics and Planetary Science*, 35, 591-599.
- Layer, P.W., Hall, C.M., York, D., 1987, The derivation of  $^{40}\text{Ar}/^{39}\text{Ar}$  age spectra of single grains of hornblende and biotite by laser step heating: *Geophysical Research Letters*, 14, 757-760.
- Lozano-Santa Cruz, R., Bernal, J.P., 2005, Characterization of a new set of eight geochemical reference materials for XRF major and trace elements analysis: *Revista Mexicana de Ciencias Geológicas*, 14 (3), 329-359.
- Ludwig, K.R., 2008, User's manual for Isoplot 3.70: a geochronological toolkit for Microsoft Excel: Berkeley Geochronology Center, Special Publication (4), 77 pp.
- Ludwig, K., R., Mundil, R., 2002, Extracting reliable U-Pb ages and errors from complex populations of zircons from Phanerozoic tuffs, in 12th Goldschmidt Conference: *Geochimica et Cosmochimica Acta*, 66, p. 463.
- Malfait, B.T., Dinkelman, M.G., 1972, Circum-Caribbean tectonic igneous activity and evolution of the Caribbean Plate: *Geological Society of America Bulletin*, 83, 251-272.
- Martini, M., Ferrari, L., López-Martínez, M., Cerca-Martínez, M., Valencia, V., Serrano-Duran, L., 2009, Cretaceous-Eocene magmatism and Laramide deformation in south-western Mexico: No role for terrane accretion, in Kay, S.M., Ramos, V.A., Dickinson, W.R. (eds.), *Backbone of the Americas: Shallow Subduction, Plateau Uplift, and Ridge and Terrane Collision*: Geological Society of America Memoir, 204, 151-182.
- Martini, M., Ferrari, L., López-Martínez, M., Valencia, V., 2010, Stratigraphic redefinition of the Zihuatanejo area, southwestern Mexico: *Revista Mexicana de Ciencias Geológicas*, 27 (3), 412-430.
- Martini, M., Mori, L., Solari, L., Centeno-García, E., 2011, Sandstone Provenance of the Arperos Basin (Sierra de Guanajuato, Central Mexico): Late Jurassic-Early Cretaceous Back-Arc Spreading as the Foundation of the Guerrero Terrane: *The Journal of Geology*, 119 (6), 597-617.
- Martini, M., Solari, L., López-Martínez, M., 2014, Correlating the Arperos Basin from Guanajuato, central Mexico, to Santo Tomás, southern Mexico: Implications for the paleogeography and origin of the Guerrero terrane: *Geosphere*, 10 (6), 1385-1401.
- McDonough, W.F., Sun, S.S., 1995, The composition of the Earth: *Chemical Geology*, 120, 223-253.
- Mendoza, O., Suástegui, M.G., 2000, Geochemistry and isotopic composition of the Guerrero Terrane (western México): Implications for the tectonomagmatic evolution of southwestern North America during the Late Mesozoic: *Journal of South American Earth Sciences*, 13, 297-324.
- Meschede, M., 1986, A method of discriminating between different types of mid-ocean ridge basalts and continental tholeiites with the Nb-Zr-Y diagram: *Chemical Geology*, 56, 207-218.
- Michaud, F., Barrier, E., Geysant, J. F., Bourgeois, J., 1987, Una serie de plataforma Mesozoica (Tithoniano Cretácico Superior) en el Estado de Colima, oeste de México: Linares, N.L., Mexico, Universidad Autónoma de Nuevo León, *Actas de la Facultad Ciencias Tierra*, 2, 63-65.
- Morán-Zenteno, D.J., Tolson, G., Martínez-Serrano, R.G., Martiny, B., Schaaf, P., Silva-Romo, G., Macías-Romo, C., Alba-Aldave, L., Hernández-Bernal, M. S., Solís-Pichardo, G., 1999, Tertiary arc magmatism of the Sierra Madre del Sur, Mexico, and its transition to the volcanic activity of the Trans-Mexican Volcanic Belt: *Journal of South American Earth Sciences*, 12, 513 - 535.
- Morán-Zenteno, D.J., Martiny, B., Tolson, G., Solís-Pichardo, G., Alba-Aldave, L., Hernández-Bernal, M.S., Macías-Romo, C., Martínez-Serrano, R.G., Schaaf, P., 2000, Geocronología y características geoquímicas de las rocas magmáticas terciarias de la Sierra Madre del Sur: *Sociedad Geológica Mexicana, Boletín*, LIII, 27-58.
- Morán-Zenteno, D.J., Alba-Aldave, L.A., Solé, J., Iriondo, A., 2004, A major resurgent caldera in southern Mexico: the source of the late Eocene Tilzapotla ignimbrite: *Journal of Volcanology and Geothermal Research*, 136, 97-116.
- Morán-Zenteno, D.J., Cerca, M., Keppie, J.D., 2005, La evolución tectónica y magmática cenozoica del suroeste de México: avances y problemas de interpretación: *Sociedad Geológica Mexicana, Boletín*, 57 (3), 319-341.
- Mori, L., Gómez-Tuena, A., Cai, Y., Goldstein, S.L., 2007, Effects of prolonged flat subduction on the Miocene magmatic record of the central Trans-Mexican Volcanic Belt: *Chemical Geology*, 244, 452-473.
- Pano, A.A., 1975, Estudio geológico del área del Estado de Colima y partes del Estado de Jalisco y Michoacán: *Petróleos Mexicanos*, reporte interno (unpublished).
- Panseri, M., 2007, Il Batolite di Manzanillo (Messico sud-occidentale): Analisi Strutturale, Petrologia, Geochimica e Geocronologia: Milano, Dottorato di Ricerca XX Ciclo Scienze della Terra, Università degli studi di Milano-Bicocca, Ph.D. Thesis, 122 pp.
- Pantoja-Alor, J., 1983, Geocronometría del magmatismo Cretácico-Terciario de la Sierra Madre del Sur: *Sociedad Geológica Mexicana, Boletín*, 44 (1), 1-20.
- Pantoja-Alor, J., Estrada-Barraza S., 1986, Estratigrafía de los alrededores de la mina de fierro de El Encino, Jalisco: *Boletín de la Sociedad Geológica Mexicana*, 47 (1), 1-15.
- Parga, M.J., 1977, Prospecto Tecmán-Colima: *Petróleos Mexicanos*, reporte interno (unpublished).
- Pearce, J.A., Harris N.B.W., Tindle A.G., 1984, Trace element discrimination diagrams for the tectonic interpretation of granitic rocks: *Journal of Petrology*, 25, 956-983.
- Peccerillo, R., Taylor S.R., 1976, Geochemistry of Eocene calc-alkaline volcanic rocks from the Kastamonu area, northern Turkey: *Contributions to Mineralogy and Petrology*, 58, 63-81.
- Petrelli M., Poli G., Perugini D., Peccerillo A., 2005, Petrograph: a new software to visualize, model, and present geochemical data in igneous petrology: *Geochemistry, Geophysics, Geosystems*, 6, Q07011.
- Pimentel, R.A., 1980, Prospecto Soyatlán de Adentro: *Petróleos Mexicanos*, IGPR-191, reporte interno (no publicado).
- Pitcher, W.S., 1982, Granite type and tectonic environment, in Hsü, K. (Ed.), *Mountain Building Processes*: London, Academic Press, 19-40.
- Plank, T., Langmuir, C., 1998, The chemical composition of subducting sediments and its consequences for the crust and mantle: *Chemical Geology*, 145, 325-394.
- Pompa-Mera, V., Schaaf, P., Hernández-Treviño, T., Weber, B., Solís-Pichardo, G., Villanueva-Lascurain, D., Layer, P., 2013, Geology, geochronology, and geochemistry of Isla María Madre, Nayarit, Mexico: *Revista Mexicana de Ciencias Geológicas*, 30 (1), 1-23.
- Ragland, P.C., 1989, *Basic Analytical Petrology*: Oxford University Press,

- Oxford, 369 pp.
- Rodríguez, R.D., 1980, Informe final del Prospecto Tecalitlán: Petróleos Mexicanos, IGPR-186, reporte interno (unpublished).
- Rollinson, H., 1993, Using Geochemical Data: Evaluation, Presentation, Interpretation: United Kingdom, Pearson Prentice Hall, Longman Group, 352 pp.
- Salazar-Juárez, J., 2015, Evolución magmática del complejo intrusivo de Jilotlán (Jalisco): Mexico, Universidad Nacional Autónoma de México, Posgrado de Ciencias de la Tierra, Instituto de Geología, M.Sc. Thesis, 161 pp.
- Schaaf, P., 1990, Isotopengeochemische Untersuchungen an Granitoiden Gesteinen eines aktiven Kontinentalrandes. Alter und Herkunft der Tiefengesteinskomplexe an der Pazifikküste Mexikos zwischen Puerto Vallarta und Acapulco: München, Ludwig-Maximilians Universität, Dissertation, 202 pp.
- Schaaf, P., 2002, Geología y Geofísica de la costa de Jalisco, *in* Noguera, F.A., Vega-Rivera J.H., García Andrete, A.N., Quesada Avendaño, M. (eds.), Historia Natural de Chamela: Universidad Nacional Autónoma de México, Instituto de Biología, 11-16.
- Schaaf, P., Heinrich, W., Besch, T., 1994, Composition and Sm-Nd isotopic data of the lower crust beneath San Luis Potosí, central Mexico: Evidence from a granulite-facies xenolith suite: *Chemical Geology*, 118, 63-84.
- Schaaf, P., Morán-Zenteno D.J., Hernández, M.S., Solís-Pichardo, G., Tolson, G., Köhler, H., 1995, Paleogene continental margin truncation in southwestern Mexico: Geochronological evidence: *Tectonics*, 14, 1339-1350.
- Schaaf, P., Böhnel, H., Pérez-Venzor, J.A., 2000, Pre-Miocene palaeogeography of the Los Cabos Block, Baja California Sur: Geochronological and palaeomagnetic constraints: *Tectonophysics*, 318, 53-69.
- Sedlock, R.L., Ortega-Gutiérrez, F., Speed, R.C., 1993, Tectonostratigraphic Terranes and Tectonic Evolution of Mexico: Geological Society of America, Special Paper, 278, 153 pp.
- Shaw, D.M., 1970, Trace element fractionation during anatexis: *Geochimica et Cosmochimica Acta*, 34, 237-243.
- Shaw, D.M., 2007, Trace Elements in Magmas: a Theoretical Treatment: USA, Cambridge University Press, 243 pp.
- Sun, S.S., McDonough, W.F., 1989, Chemical and isotopic systematics of oceanic basalts: implications for mantle composition and processes: *in* Saunders, A.D. Norry, M.J. (eds.) Magmatism in ocean basins: Geological Society, London, Special Publication, 42, 313-345.
- Talavera-Mendoza, O., 1993, Les formations orogéniques mésozoïques du Guerrero (Mexique méridional): Contribution à la connaissance de l'évolution géodynamique des cordillères mexicaines: France, Université Joseph Fourier-Grenoble I, Ph.D. thesis, 462 pp.
- Talavera-Mendoza, O., 2000, Mélanges in southern Mexico: geochemistry and metamorphism of Las Ollas complex (Guerrero Terrane): *Canadian Journal of Earth Sciences*, 37 (9), 1309-1320.
- Talavera-Mendoza, O., Ramirez-Espinosa, J., Guerrero-Suástegui, M., 1995, Petrology and geochemistry of the Teloloapan subterranean, a Lower Cretaceous evolved intra-oceanic island-arc: *Geofísica Internacional*, 34, 3-22.
- Talavera-Mendoza, O., Ruiz, J., Gehrels G.E., Valencia V.A., Centeno-García, E., 2007, Detrital zircons U/Pb geochronology of southern Guerrero and western Mixteca arc successions (southern Mexico): New insights for the tectonic evolution of southwestern North America during the late Mesozoic: *Journal of South American Earth Sciences*, 13, 297-324.
- Tardy, M., Lapierre, H., Freyrier, C., Coulon, C., Gill, J.B., Mercier de Lepinay, B.; Beck C.; Martínez, J.; Talavera, M.; Ortiz, E.; Stein, G.; Bourdier, J. L., Yta, M., 1994, The Guerrero suspect terrane (western Mexico) and coeval arc terranes (the Greater Antilles and the Western Cordillera of Colombia) a late Mesozoic intra-oceanic arc accreted to cratonic America during the Cretaceous: *Tectonophysics*, 234 (4), 49-73.
- Valdez-Moreno, G., 2006, Evolución geoquímica e isotópica del complejo volcánico de Colima: Mexico, Universidad Nacional Autónoma de México, Posgrado en Ciencias de la Tierra, Instituto de Geofísica, Ph.D. Thesis, 183 pp.
- Valencia, V., Ducea, M., Talavera-Mendoza, O., Gehrels, G., Ruiz, J., Shoemaker, S., 2009, U-Pb geochronology of granitoids in the northwestern boundary of the Xolapa Terrane: *Revista Mexicana de Ciencias Geológicas*, 26(1), 189-200.
- Villanueva-Lascurain, D., 2011, Petrogénesis de la parte gabroica del plutón de Jilotlán, Jalisco: Mexico, Facultad de Ingeniería, Universidad Nacional Autónoma de México, Bachelor Thesis, 210 pp.
- Von Huene, R., Scholl, D.W., 1991, Observations at convergent margins concerning sediment subduction, subduction erosion, and the growth of continental crust: *Reviews of Geophysics*, 29, 279-316.
- White, W.M., 2005, Geochemistry (online): <<http://www.imwa.info/white-geochemistry.html>>, revised: 28 of October 2005, downloaded: 20 of August 2011 (no longer available online; published by Wiley-Blackwell).
- Winter, J.D., 2001, An Introduction to Igneous and Metamorphic Petrology: USA, New Jersey, Prentice Hall, 697 pp.
- Workman, R.K., Hart, S.R., 2005, Major and trace element composition of the depleted MORB mantle (DMM): *Earth and Planetary Science Letters*, 231, 53-72.
- York, D., Hall, C.M., Yanase, Y., Hanes, J.A., Kenyon, W.J., 1981, <sup>40</sup>Ar/<sup>39</sup>Ar dating of terrestrial minerals with a continuous laser: *Geophysical Research Letters*, 8, 1136-1138.

Manuscript received: January 31, 2015

Corrected manuscript received: June, 26, 2015

Manuscript accepted: Septiembre 9, 2015